

ASTRONOMICAL INSTITUTE  
SLOVAK ACADEMY OF SCIENCES

CONTRIBUTIONS  
OF THE ASTRONOMICAL OBSERVATORY  
SKALNATÉ PLESO

• VOLUME XLIX •

Number 1



April 2019

## Editorial Board

### Editor-in-Chief

Augustín Skopal, *Tatranská Lomnica, The Slovak Republic*

### Managing Editor

Richard Komžík, *Tatranská Lomnica, The Slovak Republic*

### Editors

Drahomír Chochol, *Tatranská Lomnica, The Slovak Republic*

Július Koza, *Tatranská Lomnica, The Slovak Republic*

Aleš Kučera, *Tatranská Lomnica, The Slovak Republic*

Luboš Neslušan, *Tatranská Lomnica, The Slovak Republic*

Vladimír Porubčan, *Bratislava, The Slovak Republic*

Theodor Pribulla, *Tatranská Lomnica, The Slovak Republic*

### Advisory Board

Bernhard Fleck, *Greenbelt, USA*

Arnold Hanslmeier, *Graz, Austria*

Marian Karlický, *Ondřejov, The Czech Republic*

Tanya Ryabchikova, *Moscow, Russia*

Giovanni B. Valsecchi, *Rome, Italy*

Jan Vondrák, *Prague, The Czech Republic*

©

Astronomical Institute of the Slovak Academy of Sciences  
2019

ISSN: 1336-0337 (on-line version)

CODEN: CAOPF8

---

Editorial Office: Astronomical Institute of the Slovak Academy of Sciences  
SK - 05960 Tatranská Lomnica, The Slovak Republic

# CONTENTS

## EDITORIAL

A. Skopal, R. Komžík: <b>Editorial</b> . . . . .	5
--	---

## STARS

C.-Y. Huang: <b>Estimating the black hole mass of NGC 1313 X-1 based on the spectral and timing properties</b> . . . . .	7
M. Sekeráš, A. Skopal, S. Shugarov, N. Shagatova, E. Kundra, R. Komžík, M. Vrašťák, S. P. Peneva, E. Semkov, R. Stubbings: <b>Photometry of Symbiotic Stars - XIV</b> . . . . .	19

The Contributions of the Astronomical Observatory Skalnaté Pleso  
are available in a full version  
in the frame of ADS Abstract Service  
and can be downloaded in a usual way from the URL address:

**<http://adsabs.harvard.edu/>**

as well as from the web-site of  
the Astronomical Institute of the Slovak Academy of Sciences  
on the URL address:

**<https://www.astro.sk/caosp/>**

The journal is covered/indexed by:

**Thomson Reuters services (ISI)**

Science Citation Index Expanded (also known as SciSearch<sup>®</sup>)  
Journal Citation Reports/Science Edition

**SCOPUS**

## EDITORIAL

Dear Colleagues,

Above all, we are happy to say that our journal, Contributions of the Astronomical Observatory Skalnaté Pleso (CAOSP), is doing well after its principal re-construction in 2016. It is with pleasure that the CAOSP impact factor reached to date its highest value of 0.733 for 2017, and during 2018 we completed 4 issues.

Volume 48/1 contains contributions from the conference on "Stars with a stable magnetic field: from pre-main sequence to compact remnants", held in Brno, Czech Republic, during August, 28 – September 01, 2017. Presented contributions are devoted to the role of magnetic fields in evolution of stellar objects, as it is currently allowed by new highly accurate measurements and numerical simulations. All contributions (53) were peer reviewed and published in electronic form within seven months after the conference.

First set of regular articles was published in Volume 48/2. This issue presents modeling the long-term light curves of the asteroid (2501) Lohja, a study of highly energetic solar flare from September 10 2017, photometric observations of the dwarf nova V1006 Cyg and a numerical simulation of the moonlets motion in the binary and multiple asteroid systems.

Volume 48/3 presents contributions from the "10th International Workshop on Astronomical X-Ray Optics", held in Prague, Czech Republic, during December 4–7, 2017. In twelve papers on 110 pages, authors discussed recent and future technologies for X-ray astronomy missions.

Second set of regular articles was published in the 48/4 issue of CAOSP. It is devoted to photometric and spectroscopic observations of Supernova 2014J in M82, to a poorly studied Algol-type eclipsing binary V2247 Cyg and provides information of the meteor complex of the long-period comet C/1964 N1 (Ikeya).

During 2019 we plan to publish two issues with regular articles and two proceedings from international conferences. The first proceedings scheduled for Volume 49/2 will be from our conference, "Observing techniques, instrumentation and science for metre-class telescopes II", held in Tatranská Lomnica during September 24–28, 2018 and the second one is agreed for highlights from the conference, "Stars and their Variability, Observed from Space" to be held in Vienna, Austria, during August 19–23, 2019.

Finally, we inform you that the Editorial Board decided to stop publishing the paper version of CAOSP from January 1st, 2019. However, the paper version still can be arranged under request for proceedings from a conference.

Tatranská Lomnica, January 7, 2019

Augustín Skopal, Editor-in-Chief  
Richard Komžík, Managing Editor



# Estimating the black hole mass of NGC 1313 X-1 based on the spectral and timing properties

C.-Y. Huang

*School of Physics and Optoelectronic Engineering, Yangtze University,  
Jingzhou 434023, China (E-mail: hcy@yangtzeu.edu.cn)*

Received: September 26, 2018; Accepted: November 15, 2018

**Abstract.** The discovery of 3:2 quasi-periodic oscillations (QPOs) in the ultra-luminous X-ray source NGC 1313 X-1 suggests it harbors an intermediate-mass black hole (IMBH). We test this numerically by modelling the 3:2 QPOs and the associated X-ray spectrum based on the epicyclic resonance model and a disk-corona model with large-scale magnetic fields generated by the Cosmic Battery mechanism. The combined QPO-frequency and spectral fitting indicates that the BH mass ranges from  $2524M_{\odot}$  to  $6811M_{\odot}$  confirming its IMBH nature, and the BH spin is probably higher than  $\sim 0.3$ .

**Key words:** accretion, accretion disks – black hole physics – magnetic fields – stars: individual: NGC 1313 X-1

## 1. Introduction

Ultraluminous X-ray sources (ULXs) are non-nuclear point-like X-ray sources in nearby galaxies with luminosities greater than  $\sim 10^{39} \text{erg s}^{-1}$ . The nature of the compact objects in ULXs is still under debate. They are generally thought to be powered by the intermediate-mass ( $10^2 - 10^4 M_{\odot}$ ) black holes (IMBHs) since the luminosity exceeds the Eddington limit for a typical stellar-mass ( $\sim 10 M_{\odot}$ ) black hole (BH), where  $M_{\odot}$  is the solar mass. However, the spectral analyses based on high quality observations indicate that they may harbor stellar-mass BHs accreting at near-Eddington or super-Eddington rate (e.g. Stobbart et al., 2006; Gladstone et al., 2009; Jithesh et al., 2017). The super-Eddington phenomenon could also be explained by the beaming geometry or the relativistic beaming of jet emission (e.g. King et al., 2001; Poutanen et al., 2007; Körding et al., 2002; Freeland et al., 2006; Kuncic et al., 2007). Recently, the discovery of coherent X-ray pulsations from some ULXs indicates that the central engines are accreting neutron stars (Bachetti et al., 2014; Israel et al., 2017b; Fürst et al., 2016; Israel et al., 2017a; Koliopanos et al., 2017). See Kaaret et al. (2017) for a review. A direct mass measurement is needed to clarify the question of what are the compact objects harbored in ULXs.

Timing properties provide us an important clue to constrain the mass and spin of the compact objects. The discovery of 3:2 quasi-periodic oscillation (QPO) pairs in two ULXs indicates that they harbor IMBHs. Pasham et al. (2014) reported a 3:2 QPO pair at frequencies 5 and 3.3 Hz detected in ULX

M82 X-1 and estimated the mass of the compact object to be  $428 \pm 105 M_{\odot}$  using the inverse correlation between the BH mass and the frequencies of high-frequency QPOs (HFQPOs) observed in galactic BH X-ray binaries (BHXBs). Soon afterwards Pasham et al. (2015) detected another 3:2 QPO pair at frequencies 0.45 and 0.3 Hz in *XMM-Newton* observations of ULX NGC 1313 X-1. They found that the power density spectrum of NGC 1313 X-1 is analogous to that of BHXBs in the steep power-law (SPL) state and estimated the BH mass to be  $5000 M_{\odot}$  using the inverse mass-to-HFQPO frequency scaling.

Jang et al. (2018) applied the X-ray scaling method to measure the BH mass in ULXs with multiple X-ray observations and their estimated BH mass of NGC 1313 X-1 was in the range 295 – 6166  $M_{\odot}$ .

Both the QPO scaling and the X-ray scaling methods imply NGC 1313 X-1 harbors an IMBH. However, quantitative and numerical analyses are needed to test this result. In this paper, we estimate the BH mass in NGC 1313 X-1 by modelling the 3:2 QPOs and the associated X-ray spectrum simultaneously based on the epicyclic resonance model (ERM) and a magnetic disk-corona model developed by Huang et al. (2016).

The paper is organised as follows. In section 2, we give a description of the model. In section 3, the 3:2 QPO frequencies and the associated X-ray spectrum are fitted and the range of the BH mass is obtained. We discuss and summarize in section 4. The geometric units  $G = c = 1$  are used throughout this paper.

## 2. Model description

### 2.1. The magnetic disk-corona model

The energy transferred from the rotating BH and the plunging region to the inner disk is considered through the magnetic connection (MC) process by the large-scale magnetic fields generated by the Poynting-Robertson Cosmic Battery (PRCB) mechanism (Contopoulos & Kazanas, 1998; Contopoulos et al., 2006; Kylafis et al., 2012). In the PRCB scenario, electrons in the inner accretion disk feel a much stronger radiation-drag force than the ions due to a much larger Thompson cross-section leading to an electric current loop generated near the inner edge of the accretion disk. The current intensity can be estimated as (Huang et al., 2016)

$$I = en\Delta t\Delta S F\sigma_{\text{T}}v_{\text{k}}/m_{\text{e}}, \quad (1)$$

where  $\Delta t$  and  $\Delta S$  are the average scattering time of electrons with photons and the cross-section of the current, respectively,  $F$  is the radiation flux from the relativistic accretion disk (Novikov & Thorne, 1973; Page & Thorne, 1974),  $n$  is the number density of electrons,  $v_{\text{k}}$  is the Kepler velocity,  $\sigma_{\text{T}}$  is the Thompson cross-section and  $e$  is the electric quality of an electron. Following Huang et al. (2016), we set  $\Delta t = 10^{-9}\text{s}$  and  $\Delta S = (0.01M_{\text{BH}})^2$ , where  $M_{\text{BH}}$  is the BH mass. The values of  $F$ ,  $n$  and  $v_{\text{k}}$  are all evaluated at the radius  $r_{\text{PRCB}}$  where

the current is generated. As suggested by Kylafis et al. (2012), the current is generated near the innermost stable circular orbit (ISCO) of the disk. Fitting the 3:2 HFQPO pairs and the associated spectrum from BHXBs by Huang et al. (2016) also indicates that the current is very near the ISCO. For simplicity, We set  $r_{\text{PRCB}} = 1.01r_{\text{ISCO}}$  in this work, where  $r_{\text{ISCO}}$  is the radius of ISCO.

The magnetic fields generated by the PRCB current can be calculated in the frame of general relativity (Linet, 1979; Li, 2002b). As shown in Huang et al. (2016), two types of MC configurations are created by the PRCB current with one connecting the BH horizon and the disk and the other connecting the plunging region and the inner disk. The rotational energy of both the BH and the plunging region can be transferred to the inner disk by these two MC processes. The energy dissipated at unit disk area caused by MC is expressed as (Li, 2002a)

$$Q_{\text{MC}}^+ = r^{-1}S^{-2}\left(-\frac{d\Omega_{\text{D}}}{dr}\right)\int_{r_{\text{in}}}^r SH_{\text{MC}}rdr, \quad (2)$$

where  $S = E^\dagger - \Omega_{\text{D}}L^\dagger$  with  $E^\dagger$ ,  $L^\dagger$  and  $\Omega_{\text{D}}$  are, respectively, the specific energy, the specific angular momentum and angular velocity of a test particle in the accretion disk (Bardeen et al., 1972). In equation (2),  $H_{\text{MC}} \equiv \frac{1}{4\pi r} \frac{dT}{dr}$  is the flux of angular momentum transferred to the disk, where  $T$  is the torque exerting on the disk surface by MC (Li, 2002a), and  $r_{\text{in}}$  is the inner most disk radius receiving energy from the plunging region.

The gravitational power dissipated in unit disk surface is (Page & Thorne, 1974)

$$Q_{\text{DA}}^+ = \frac{\dot{M}}{4\pi r} f, \quad (3)$$

where  $\dot{M}$  is the mass accretion rate of the disk and  $f$  is a function of  $a_*$ ,  $r$  and  $M_{\text{BH}}$  as given in Page & Thorne (1974), where  $a_* \equiv J/M_{\text{BH}}^2$  is the dimensionless BH spin defined in terms of  $M_{\text{BH}}$  and BH angular momentum  $J$ .

The corona is assumed to be heated by the reconnection of the small-scale magnetic field that generated by the buoyancy instability in the disk (Di Matteo, 1998; Liu et al., 2002). The power dissipated in the corona is (Liu et al., 2002)

$$Q_{\text{cor}}^+ = \frac{B_{\text{d}}^2}{4\pi} v_{\text{A}}, \quad (4)$$

where  $B_{\text{d}}$  is the small-scale magnetic field in the disk, and  $v_{\text{A}} \equiv B_{\text{d}}/\sqrt{4\pi\rho}$  is the Alfvén speed, where  $\rho$  is the mass density of the disk.

Part of the energy dissipated in the disk is radiated as black body, and the other part is released into the corona. Thus, the energy equation for the disk is

$$Q_{\text{DA}}^+ + Q_{\text{MC}}^+ - Q_{\text{cor}}^+ = \frac{4\sigma T_{\text{d}}^4}{3\tau_{\text{d}}}, \quad (5)$$

where  $T_{\text{d}}$  is the temperature in the mid-plane of the disk,  $\sigma$  is the Stefan-Boltzmann constant, and  $\tau_{\text{d}}$  is the optical depth in the vertical direction of the

disk which is related to the mean opacity  $\kappa$  as

$$\tau_d = \rho h \kappa = \rho h (\kappa_{\text{ff}} + \kappa_{\text{es}}), \quad (6)$$

where  $h$  is the half-thickness of the disk,  $\kappa_{\text{ff}}$  and  $\kappa_{\text{es}}$  are the contributions of free-free transitions and electron scattering respectively, and  $\kappa_{\text{ff}} = 6.4 \times 10^{22} \rho T_d^{-7/2} \text{ cm}^2 \text{ g}^{-1}$  and  $\kappa_{\text{es}} = 0.4 \text{ cm}^2 \text{ g}^{-1}$  are adopted (Novikov & Thorne, 1973).

The equation for the vertical pressure balance of the disk is (Novikov & Thorne, 1973)

$$h = P^{1/2} \rho^{-1/2} r^{3/2} M_{\text{BH}}^{-1/2} \mathcal{A} \mathcal{B}^{-1} \mathcal{C}^{1/2} \mathcal{D}^{-1/2} \mathcal{E}^{-1/2}, \quad (7)$$

where  $P = P_{\text{gas}} + P_{\text{rad}} + P_{\text{mag}}$ , and  $P_{\text{gas}}$ ,  $P_{\text{rad}}$  and  $P_{\text{mag}}$  are, respectively, the gas pressure, radiation pressure and magnetic pressure of the disk.  $\mathcal{A}$ ,  $\mathcal{B}$ ,  $\mathcal{C}$ ,  $\mathcal{D}$  and  $\mathcal{E}$  are the relativistic correction factors in Kerr metric (Novikov & Thorne, 1973).

Magnetohydrodynamics (MHD) simulations reveal that the viscosity in the accretion disk is related to the tangled small-scale magnetic fields. However, the detailed physics of the generation of the small-scale magnetic fields is still unclear. The famous ‘ $\alpha$ -prescription’ proposed by Shakura & Sunyaev (1973) is widely used in various theoretical works. Observations favor the interior viscous stress  $t_{r\varphi}$  proportional to the gas pressure (Wang et al., 2004). Therefore we adopt this  $\alpha$ -prescription in our calculation:

$$t_{r\varphi} = P_{\text{mag}} = \frac{B_d^2}{8\pi} = \alpha P_{\text{gas}}, \quad (8)$$

where  $\alpha$  is the viscosity parameter.

The continuity equation of the disk is (Novikov & Thorne, 1973)

$$\dot{M} = -4\pi r h \rho v_r \mathcal{D}^{1/2}, \quad (9)$$

where  $v_r$  is the radial velocity of the accretion flow at radius  $r$ . Incorporating the energy and angular-momentum equations for the disk, the stress  $t_{r\varphi}$  is related to the dissipated energy as follow (Page & Thorne, 1974; Li, 2002a)

$$r h t_{r\varphi} = S \left( -\frac{d\Omega_D}{dr} \right)^{-1} (Q_{\text{DA}}^+ + Q_{\text{MC}}^+). \quad (10)$$

The equation of state for the gas in the disk is

$$P_{\text{rad}} + P_{\text{gas}} = \frac{1}{3} a_0 T_d^4 + \frac{\rho k T_d}{\mu m_p}, \quad (11)$$

where  $a_0$  is the radiation constant,  $k$  is the Boltzmann constant,  $m_p$  is the proton mass, and  $\mu = 0.615$  is adopted being the mean atomic mass.

The electrons in the corona are heated by the magnetic reconnection and are cooled via the inverse Compton scattering by the soft photons from the cold disk. Thus, the energy equation of the corona is (Liu et al., 2002)

$$Q_{\text{cor}}^+ = Q_{\text{comp}}^- = \frac{4kT_e}{m_e} \tau U_{\text{rad}}, \quad (12)$$

where  $U_{\text{rad}} = a_0 T_d^4$  is the energy density of the soft photon field,  $T_e$  is the temperature of the corona,  $m_e$  is the electron mass, and  $\tau$  is the optical depth of the corona.

Following Huang et al. (2016), we take the optical depth, the height and the outer boundary of the corona as  $\tau = 1$ ,  $l = 20M_{\text{BH}}$  and  $r_{\text{out}} = 100M_{\text{BH}}$ , respectively. Solving equations (1) – (12) numerically, we can obtain the global solutions of the disk-corona system with MC process. The X-ray spectrum of the system can be simulated using Monte Carlo method (Gan et al., 2009).

## 2.2. The 3:2 QPO model

There is no consensus on the mechanism of QPO generation although a variety of models have been proposed (see Belloni & Stella, 2014, for a review). We interpret 3:2 QPO pairs based on ERM (Abramowicz & Kluźniak, 2001) since it naturally explains the small integer ratios of 3:2 QPO frequencies.

In the general relativistic frame, a test particle in the equatorial plane around a compact object has three basic oscillation frequencies, namely, the orbital frequency  $\nu_\phi$ , the vertical epicyclic frequency  $\nu_\theta$  and the radial epicyclic frequency  $\nu_r$ , which are functions of  $a_*$ ,  $r$  and  $M_{\text{BH}}$  given as follows (Bardeen et al., 1972; Okazaki et al., 1987; Kato, 1990; van der Klis, 2006)

$$\nu_\phi = [2\pi M_{\text{BH}}(\tilde{r}^{3/2} + a_*)]^{-1}, \quad (13)$$

$$\nu_\theta = \nu_\phi(1 - 4a_*\tilde{r}^{-3/2} + 3a_*^2\tilde{r}^{-2})^{1/2}, \quad (14)$$

$$\nu_r = \nu_\phi(1 - 6\tilde{r}^{-1} + 8a_*\tilde{r}^{-3/2} - 3a_*^2\tilde{r}^{-2})^{1/2}, \quad (15)$$

where  $\tilde{r} \equiv r/M_{\text{BH}}$ .

In ERM, resonances occur at specific radii of the disk if the vertical and the radial epicyclic frequencies have small integer ratios resulting in oscillations of the plasmoid. As argued by Huang et al. (2010, 2016), the severe damping forces on the oscillations can be overcome by transferring energy from the spinning BH to the inner disk via the MC process therefore the resonances persist and emit X-rays with sufficient amplitude and coherence to produce the observed QPOs.

Applying to NGC 1313 X-1, we treat the frequency of the 0.45 Hz QPO as  $\nu_\theta$  and the 0.3 Hz as  $\nu_r$ . For a given BH spin, the BH mass and the resonance radius  $\tilde{r}_{\text{res}}$  can be obtained by solving the equations

$$\begin{cases} \nu_\theta/\nu_r = 3/2, \\ \nu_\theta = 0.45. \end{cases} \quad (16)$$

**Table 1.** Parameters for fitting the 3:2 QPO frequencies and the associated X-ray spectrum.

$a_*$	$m_{\text{BH}}$	$\tilde{r}_{\text{res}}$	$\dot{m}$	$\alpha$	$n_{\text{H}}(10^{22}\text{cm}^{-2})$
0.3	2524	9.13	0.38	0.39	0.45
0.998	6811	3.89	0.00032	0.22	0.28

### 3. Fitting the 3:2 QPO frequencies and the associated X-ray spectrum

The 0.45 and 0.3 Hz QPOs of NGC 1313 X-1 were detected simultaneously on 2012 December 16 in the *XMM-Newton* observation (obsID: 0693850501) at energy band of 0.3 – 10 keV (Pasham et al., 2015). We first fit the 3:2 QPO frequencies and then fit the 0.3 – 10 keV spectrum from this *XMM-Newton* observation.

In the spectral simulation, the distance to the source  $d = 4.61\text{Mpc}$  (Qing et al., 2015) is adopted and the inclination  $i$  of the system is assumed to be  $70^\circ$  for an analogy with the X-ray binary systems since almost all the BHXBs displaying HFQPOs have high inclinations (Miller & Miller, 2015), which is close to the values ( $66^\circ - 76^\circ$ ) obtained by spectral fitting models of Bachetti et al. (2013).

Since the BH spin of NGC 1313 X-1 has not been measured, we consider two extremes, the Schwarzschild BH with  $a_* = 0$  and the extreme Kerr BH with  $a_* = 0.998$ . The corresponding lower and upper limits of the BH mass obtained by solving equation (16) are  $2024M_\odot$  and  $6811M_\odot$ , respectively. Based on the values of  $m_{\text{BH}}$  ( $m_{\text{BH}} \equiv M_{\text{BH}}/M_\odot$ ) and  $a_*$ , we then fit the spectrum by adjusting the parameters  $\dot{m}$ ,  $\alpha$  and  $n_{\text{H}}$ , where  $\dot{m} \equiv \dot{M}/\dot{M}_{\text{Edd}}$  and  $\dot{M}_{\text{Edd}} \simeq 1.4 \times 10^{18} m_{\text{BH}} \text{ g s}^{-1}$  is the Eddington accretion rate, and  $n_{\text{H}}$  is the hydrogen column density.

It turns out that a larger BH mass leads to a better spectral fitting and the spectrum can not be fitted well if  $a_* \lesssim 0.3$  since the BH mass is too small. The parameters corresponding to the lower and upper limits of the values of  $a_*$  and  $m_{\text{BH}}$  for fitting the 3:2 QPO frequencies and the associated X-ray spectrum are listed in Table 1. The corresponding simulated spectra are plotted in Fig. 1, which fit very well into the observed one in the 0.5 – 10 keV band. The deviation below 0.5 keV may be due to that we do not consider the synchrotron and bremsstrahlung radiation from the corona in our model.

The simulated spectrum is more sensitive to  $\dot{m}$  for a larger  $a_*$  due to the stronger MC effect by the large-scale magnetic fields generated by PRCB current which is proportional to  $\dot{m}$  as indicated by equation (3).

Inspecting Table 1, one can find that a larger BH mass is needed to fit the 3:2 QPO frequencies for a higher BH spin. And larger values of  $\dot{m}$  and  $\alpha$  are needed

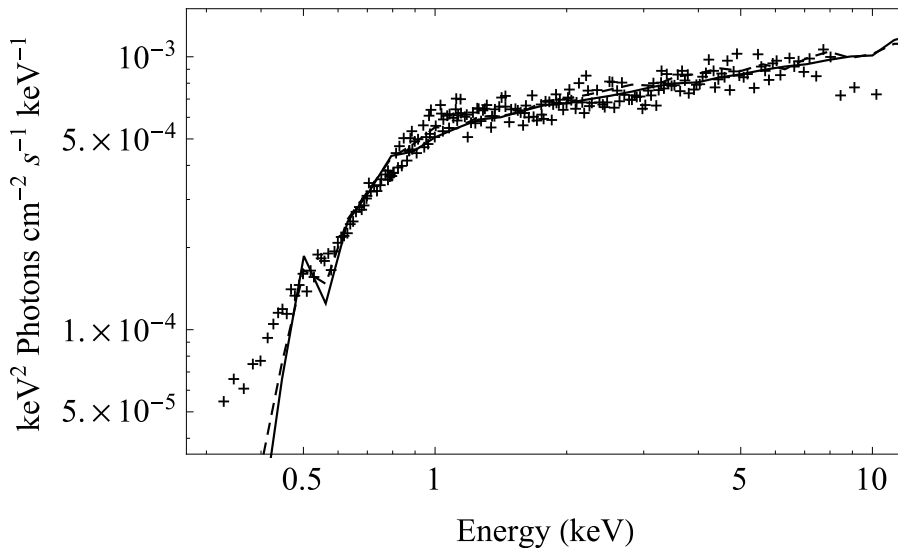


**Figure 1.** The simulated and observed spectra of NGC 1313 X-1 associated with the 3:2 QPOs. The solid and dashed lines represent the model spectra with  $a_* = 0.3$  and  $a_* = 0.998$ , respectively. The symbol “+” denotes the observed spectrum (without error bars) with data taken from Bachetti et al. (2013).

to fit the spectrum for a lower BH spin and a smaller BH mass, which means both the soft component, which is proportional to  $\dot{m}$  as indicated by equation (3), and the hard component, which is proportional to  $\alpha$  as indicated by equation (8) and equation (4), should be enhanced to fit the observed spectrum.

#### 4. Summary and discussion

In this paper, we modelled the 0.45 and 0.3 Hz QPOs and the associated 0.3 – 10 keV X-ray spectrum of NGC 1313 X-1 based on ERM and a disk-corona model with PRCB. The combined QPO-frequency and spectral fitting indicates that the BH mass lies in the range  $2524 - 6811M_\odot$  and the BH spin is probably higher than  $\sim 0.3$ . This is the first time to model the combined spectral and timing properties of NGC 1313 X-1 numerically and self-consistently. The result confirms that NGC 1313 X-1 contains an IMBH consistent with the results of Pasham et al. (2015) and Jang et al. (2018).

We find that the magnetic fields play an important role in the spectral fitting. The simulated spectra are in accordance with the observed one only when the intensity of the magnetic fields at  $r_{\text{ISCO}}$  generated by PRCB is comparable to that at the BH horizon evaluated by the balance of the ram pressure and the

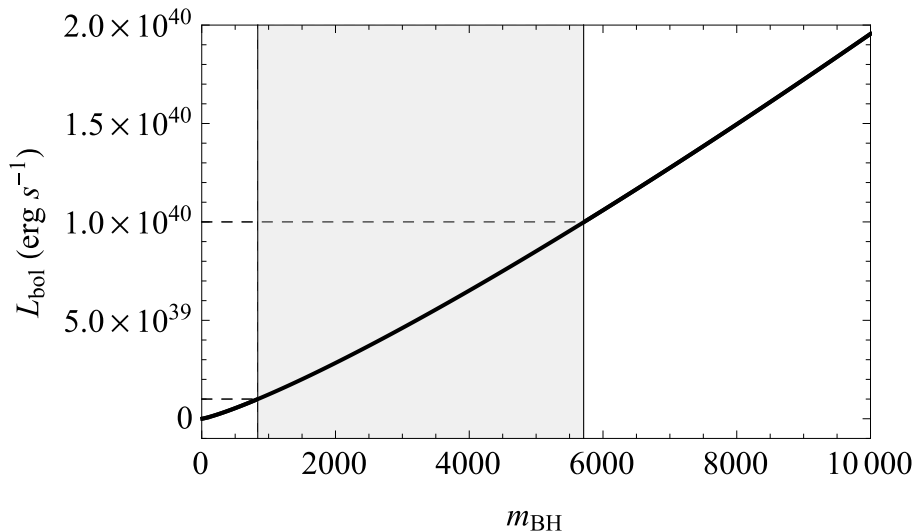


**Figure 2.** The curve of the bolometric luminosity as a function of BH mass for the PRCB magnetic fields at ISCO become saturated. The shaded area indicates the BH mass ranges between  $839M_{\odot}$  and  $5719M_{\odot}$  for the bolometric luminosity ranges from  $10^{39}$  to  $10^{40}$  erg s $^{-1}$ .

magnetic pressure. This means that the magnetic fields become saturated and the disk is in the magnetically arrested disk (MAD) state (Igumenshchev et al., 2003). Our model suggests that ULXs especially those brightest, like NGC 1313 X-1, may be close to or reach the MAD state. If this is indeed the case, we can predict the bolometric luminosity of an ULX by figuring out the accretion rate to make the magnetic fields become saturated for a given BH mass, or, conversely, the BH mass can be obtained with the saturated magnetic fields for a given bolometric luminosity.

Let's make a simple estimate. For  $a_* = 0.9$  and  $\alpha = 0.3$ , the intensity of the PRCB magnetic fields  $B_{\text{PRCB}}$  at  $r_{\text{ISCO}}$  in our model can be expressed as

$$B_{\text{PRCB}} = 4.5 \times 10^7 \left( \frac{\dot{m}}{0.1} \right)^{1.5} \left( \frac{m_{\text{BH}}}{5000} \right)^{-0.7} \text{ Gauss.} \quad (17)$$

The MAD magnetic fields can be estimated by the balance of the ram pressure of the innermost part of the accretion flow and the magnetic pressure on the BH horizon (Moderski et al., 1997; Wang et al., 2002; Gan et al., 2009):

$$B_{\text{MAD}} = \sqrt{2\dot{M}/r_{\text{H}}} = 6.1 \times 10^6 \left( \frac{\dot{m}}{0.1} \right)^{0.5} \left( \frac{m_{\text{BH}}}{5000} \right)^{-0.5} \text{ Gauss,} \quad (18)$$

where  $r_{\text{H}} = M_{\text{BH}}(1 + \sqrt{1 - a_*^2})$  is the radius of the BH horizon. Assuming the radiation efficiency  $\eta = 0.1$  and the bolometric luminosity  $L_{\text{bol}} = \eta \dot{M}$ , let  $B_{\text{PRCB}} = B_{\text{MAD}}$ , we have

$$L_{\text{bol}} = 8.5 \times 10^{39} \left( \frac{m_{\text{BH}}}{5000} \right)^{1.2} \text{ erg s}^{-1}. \quad (19)$$

If  $L_{\text{bol}}$  is between  $10^{39}$  and  $10^{40}$  erg s $^{-1}$ , then the constrained BH mass is between  $839M_{\odot}$  and  $5719M_{\odot}$ , as indicated by the grey shaded area in Fig. 2.

In the spectral fitting, we only considered the 0.3 – 10 keV *XMM-Newton* spectrum associated with the 3:2 QPOs. The *NuSTAR* spectrum shows a clear cutoff above 10 keV and decays up to  $\sim 30$  keV, which can be described by a phenomenological model that includes a multi-color disk plus a two-component corona composed of a cold, optically thick medium and a second, hot and optically thin one (Bachetti et al., 2013). We will improve our model by considering multi-temperature corona with different geometries (e.g. spherical corona, “lamp-post” corona) in future works to understand both the *XMM-Newton* and *NuSTAR* spectra and to obtain more accurate and reliable measurements for the BH mass and spin of NGC 1313 X-1 and other BH systems.

**Acknowledgements.** This work has been supported by the National Natural Science Foundation of China (Grant No.11403003). We thank the anonymous referee for his (her) helpful suggestion.

## References

- Abramowicz, M. A. & Kluźniak, W., A precise determination of black hole spin in GRO J1655-40. 2001, *Astron. Astrophys.*, **374**, L19, DOI: 10.1051/0004-6361:20010791
- Bachetti, M., Harrison, F. A., Walton, D. J., et al., An ultraluminous X-ray source powered by an accreting neutron star. 2014, *Nature*, **514**, 202, DOI: 10.1038/nature13791
- Bachetti, M., Rana, V., Walton, D. J., et al., The Ultraluminous X-Ray Sources NGC 1313 X-1 and X-2: A Broadband Study with NuSTAR and XMM-Newton. 2013, *Astrophys. J.*, **778**, 163, DOI: 10.1088/0004-637X/778/2/163
- Bardeen, J. M., Press, W. H., & Teukolsky, S. A., Rotating Black Holes: Locally Non-rotating Frames, Energy Extraction, and Scalar Synchrotron Radiation. 1972, *Astrophys. J.*, **178**, 347, DOI: 10.1086/151796
- Belloni, T. M. & Stella, L., Fast Variability from Black-Hole Binaries. 2014, *Space Sci. Rev.*, **183**, 43, DOI: 10.1007/s11214-014-0076-0
- Contopoulos, I. & Kazanas, D., A Cosmic Battery. 1998, *Astrophys. J.*, **508**, 859, DOI: 10.1086/306426
- Contopoulos, I., Kazanas, D., & Christodoulou, D. M., The Cosmic Battery Revisited. 2006, *Astrophys. J.*, **652**, 1451, DOI: 10.1086/507600

- Di Matteo, T., Magnetic reconnection: flares and coronal heating in active galactic nuclei. 1998, *Mon. Not. R. Astron. Soc.*, **299**, L15, DOI: 10.1046/j.1365-8711.1998.01950.x
- Freeland, M., Kuncic, Z., Soria, R., & Bicknell, G. V., Radio and X-ray properties of relativistic beaming models for ultraluminous X-ray sources. 2006, *Mon. Not. R. Astron. Soc.*, **372**, 630, DOI: 10.1111/j.1365-2966.2006.10750.x
- Fürst, F., Walton, D. J., Harrison, F. A., et al., Discovery of Coherent Pulsations from the Ultraluminous X-Ray Source NGC 7793 P13. 2016, *Astrophys. J., Lett.*, **831**, L14, DOI: 10.3847/2041-8205/831/2/L14
- Gan, Z.-M., Wang, D.-X., & Lei, W.-H., A model of magnetically induced disc-corona for black hole binaries. 2009, *Mon. Not. R. Astron. Soc.*, **394**, 2310, DOI: 10.1111/j.1365-2966.2009.14518.x
- Gladstone, J. C., Roberts, T. P., & Done, C., The ultraluminous state. 2009, *Mon. Not. R. Astron. Soc.*, **397**, 1836, DOI: 10.1111/j.1365-2966.2009.15123.x
- Huang, C.-Y., Gan, Z.-M., Wang, J.-Z., & Wang, D.-X., A resonance model with magnetic connection for 3:2 HFQPO pairs in black hole binaries. 2010, *Mon. Not. R. Astron. Soc.*, **403**, 1978, DOI: 10.1111/j.1365-2966.2009.16237.x
- Huang, C.-Y., Ye, Y.-C., Wang, D.-X., & Li, Y., A model for 3:2 HFQPO pairs in black hole binaries based on cosmic battery. 2016, *Mon. Not. R. Astron. Soc.*, **457**, 3859, DOI: 10.1093/mnras/stw226
- Igumenshchev, I. V., Narayan, R., & Abramowicz, M. A., Three-dimensional Magnetohydrodynamic Simulations of Radiatively Inefficient Accretion Flows. 2003, *Astrophys. J.*, **592**, 1042, DOI: 10.1086/375769
- Israel, G. L., Belfiore, A., Stella, L., et al., An accreting pulsar with extreme properties drives an ultraluminous x-ray source in NGC 5907. 2017a, *Science*, **355**, 817, DOI: 10.1126/science.aai8635
- Israel, G. L., Papitto, A., Esposito, P., et al., Discovery of a 0.42-s pulsar in the ultraluminous X-ray source NGC 7793 P13. 2017b, *Mon. Not. R. Astron. Soc.*, **466**, L48, DOI: 10.1093/mnrasl/slw218
- Jang, I., Gliozzi, M., Satyapal, S., & Titarchuk, L., Measuring the black hole mass in ultraluminous X-ray sources with the X-ray scaling method. 2018, *Mon. Not. R. Astron. Soc.*, **473**, 136, DOI: 10.1093/mnras/stx2178
- Jithesh, V., Misra, R., & Wang, Z., Long-term Spectral Variability of the Ultraluminous X-Ray Source Holmberg IX X-1. 2017, *Astrophys. J.*, **849**, 121, DOI: 10.3847/1538-4357/aa8eeb
- Kaaret, P., Feng, H., & Roberts, T. P., Ultraluminous X-Ray Sources. 2017, *Ann. Rev. Astron. Astrophys.*, **55**, 303, DOI: 10.1146/annurev-astro-091916-055259
- Kato, S., Trapped one-armed corrugation waves and QPOs. 1990, *Publ. Astron. Soc. Jap.*, **42**, 99
- King, A. R., Davies, M. B., Ward, M. J., Fabbiano, G., & Elvis, M., Ultraluminous X-Ray Sources in External Galaxies. 2001, *Astrophys. J., Lett.*, **552**, L109, DOI: 10.1086/320343

- Koliopanos, F., Vasilopoulos, G., Godet, O., et al., ULX spectra revisited: Accreting, highly magnetized neutron stars as the engines of ultraluminous X-ray sources. 2017, *Astron. Astrophys.*, **608**, A47, DOI: 10.1051/0004-6361/201730922
- Körding, E., Falcke, H., & Markoff, S., Population X: Are the super-Eddington X-ray sources beamed jets in microblazars or intermediate mass black holes? 2002, *Astron. Astrophys.*, **382**, L13, DOI: 10.1051/0004-6361:20011776
- Kuncic, Z., Soria, R., Hung, C. K., Freeland, M. C., & Bicknell, G. V., Ultra-luminous X-ray sources: X-ray binaries in a high/hard state? 2007, in IAU Symposium, Vol. **238**, *Black Holes from Stars to Galaxies – Across the Range of Masses*, ed. V. Karas & G. Matt, 247–250
- Kylafis, N. D., Contopoulos, I., Kazanas, D., & Christodoulou, D. M., Formation and destruction of jets in X-ray binaries. 2012, *Astron. Astrophys.*, **538**, A5, DOI: 10.1051/0004-6361/201117052
- Li, L.-X., Accretion Disk Torqued by a Black Hole. 2002a, *Astrophys. J.*, **567**, 463, DOI: 10.1086/338486
- Li, L.-X., Toy model for the magnetic connection between a black hole and a disk. 2002b, *Phys. Rev. D*, **65**, 084047, DOI: 10.1103/PhysRevD.65.084047
- Linet, B., Stationary axisymmetric electromagnetic fields in the Kerr metric. 1979, *Journal of Physics A Mathematical General*, **12**, 839, DOI: 10.1088/0305-4470/12/6/013
- Liu, B. F., Mineshige, S., & Shibata, K., A Simple Model for a Magnetic Reconnection-heated Corona. 2002, *Astrophys. J., Lett.*, **572**, L173, DOI: 10.1086/341877
- Miller, M. C. & Miller, J. M., The masses and spins of neutron stars and stellar-mass black holes. 2015, *Physics Reports*, **548**, 1, DOI: 10.1016/j.physrep.2014.09.003
- Moderski, R., Sikora, M., & Lasota, J. P., On Black Hole Spins and Dichotomy of Quasars. 1997, in *Relativistic Jets in AGNs*, ed. M. Ostrowski, M. Sikora, G. Madejski, & M. Begelman, 110–116
- Novikov, I. D. & Thorne, K. S., Astrophysics of black holes. 1973, in *Black Holes (Les Astres Occlus)*, ed. C. Dewitt & B. S. Dewitt, 343–450
- Okazaki, A. T., Kato, S., & Fukue, J., Global trapped oscillations of relativistic accretion disks. 1987, *Publ. Astron. Soc. Jap.*, **39**, 457
- Page, D. N. & Thorne, K. S., Disk-Accretion onto a Black Hole. Time-Averaged Structure of Accretion Disk. 1974, *Astrophys. J.*, **191**, 499, DOI: 10.1086/152990
- Pasham, D. R., Cenko, S. B., Zoghbi, A., et al., Evidence for High-frequency QPOs with a 3:2 Frequency Ratio from a 5000 Solar Mass Black Hole. 2015, *Astrophys. J., Lett.*, **811**, L11, DOI: 10.1088/2041-8205/811/1/L11
- Pasham, D. R., Strohmayer, T. E., & Mushotzky, R. F., A 400-solar-mass black hole in the galaxy M82. 2014, *Nature*, **513**, 74, DOI: 10.1038/nature13710
- Poutanen, J., Lipunova, G., Fabrika, S., Butkevich, A. G., & Abolmasov, P., Super-critically accreting stellar mass black holes as ultraluminous X-ray sources. 2007, *Mon. Not. R. Astron. Soc.*, **377**, 1187, DOI: 10.1111/j.1365-2966.2007.11668.x

- Qing, G., Wang, W., Liu, J.-F., & Yoachim, P., The Distance Measurement of NGC 1313 with Cepheids. 2015, *Astrophys. J.*, **799**, 19, DOI: 10.1088/0004-637X/799/1/19
- Shakura, N. I. & Sunyaev, R. A., Black holes in binary systems. Observational appearance. 1973, *Astron. Astrophys.*, **24**, 337
- Stobbart, A. M., Roberts, T. P., & Wilms, J., XMM-Newton observations of the brightest ultraluminous X-ray sources. 2006, *Mon. Not. R. Astron. Soc.*, **368**, 397, DOI: 10.1111/j.1365-2966.2006.10112.x
- van der Klis, M. 2006, *Rapid X-ray Variability*, ed. W. H. G. Lewin & M. van der Klis, 39–112
- Wang, D. X., Xiao, K., & Lei, W. H., Evolution characteristics of the central black hole of a magnetized accretion disc. 2002, *Mon. Not. R. Astron. Soc.*, **335**, 655, DOI: 10.1046/j.1365-8711.2002.05652.x
- Wang, J.-M., Watarai, K.-Y., & Mineshige, S., The Hot Disk Corona and Magnetic Turbulence in Radio-quiet Active Galactic Nuclei: Observational Constraints. 2004, *Astrophys. J., Lett.*, **607**, L107, DOI: 10.1086/421906

## Photometry of Symbiotic Stars - XIV

M. Sekeráš<sup>1</sup>, A. Skopal<sup>1</sup>, S. Shugarov<sup>1,2</sup>, N. Shagatova<sup>1</sup>, E. Kundra<sup>1</sup>,  
R. Komžík<sup>1</sup>, M. Vrašťák<sup>3</sup>, S. P. Peneva<sup>4</sup>, E. Semkov<sup>4</sup> and  
R. Stubbings<sup>5</sup>

<sup>1</sup> *Astronomical Institute of the Slovak Academy of Sciences  
059 60 Tatranská Lomnica, The Slovak Republic, (E-mail: skopal@ta3.sk)*

<sup>2</sup> *P. K. Sternberg Astronomical Institute, M. V. Lomonosov Moscow State  
University, Russia*

<sup>3</sup> *Private observatory, 03401 Liptovská Štiavnica, The Slovak Republic*

<sup>4</sup> *Institute of Astronomy and National Astronomical Observatory, Bulgarian  
Academy of Sciences, 72 Tsarigradsko Shose Blvd., BG-1784 Sofia, Bulgaria*

<sup>5</sup> *Tetoora Observatory, 2643 Warragul-Korumburra Road, Tetoora Road,  
Victoria 3821, Australia*

Received: March 22, 2019; Accepted: April 2, 2019

**Abstract.** We present new multicolour  $UBVR_CI_C$  photometric observations of symbiotic stars, EG And, Z And, BF Cyg, CH Cyg, CI Cyg, V1016 Cyg, V1329 Cyg, AG Dra, RS Oph, AG Peg, AX Per, and the newly discovered (August 2018) symbiotic star HBHA 1704-05, we carried out during the period from 2011.9 to 2018.75. Historical photographic and visual/ $V$  data were collected for HBHA 1704-05, FG Ser and AE Ara, AR Pav, respectively. The main aim of this paper is to present our original observations of symbiotic stars and to describe the most interesting features of their light curves. For example, periodic variations, rapid variability, minima, eclipses, outbursts, apparent changes of the orbital period, etc. Our measurements were obtained by the classical photoelectric photometry (till 2016.1) and the CCD photometry. Main results of our monitoring program are summarized and some specific characteristics are pointed out for future investigation.<sup>1</sup>

**Key words:** catalogs – binaries: symbiotics – techniques: photometric

### 1. Introduction

Symbiotic stars are the widest interacting binary systems that comprise a cool giant as the donor and a white dwarf (WD) accreting from the giant's wind (Boyarchuk, 1967; Kenyon, 1986; Mürset & Schmid, 1999). Their orbital periods run from hundreds of days (S-type systems containing a normal giant) to a few times 10–100 years (D-type systems containing a Mira variable)<sup>2</sup>. The former case is given by our knowledge of the photometric and/or spectroscopic orbital

<sup>1</sup>on-line data: <http://www.astro.sk/caosp/Eedition/FullTexts/vol49no1/pp19-66.dat/>

<sup>2</sup>see Webster & Allen (1975) for details of this classification

elements (e.g. Belczyński *et al.*, 2000), while the latter is based on the long-term spectroscopic observations and/or imaging (e.g. Parimucha *et al.*, 2002; Matthews & Karovska, 2006). However, they are, in general, unknown.

The accreting WD represents a strong source of the supersoft X-ray to UV radiation ( $T_{\text{WD}} \gtrsim 10^5$  K,  $L_{\text{WD}} \sim 10^1 - 10^4 L_{\odot}$ ) in the binary (Muerstet *et al.*, 1991; Skopal, 2005; Skopal *et al.*, 2009; González-Riestra *et al.*, 2013; Ramsay *et al.*, 2016; Skopal *et al.*, 2017b) that ionizes a fraction of the wind from the giant giving rise to the nebular emission (e.g. Boyarchuk *et al.*, 1966; Seaquist *et al.*, 1984; Kenyon & Webbink, 1984; Nussbaumer & Vogel, 1987). This configuration represents the so-called *quiescent phase* of symbiotic binary, during which the symbiotic system releases its energy approximately at a constant rate and temperature. Corresponding optical light curves (LC) are characterized with a well pronounced periodic wave-like variation along the orbit. Analyses and discussions of this fundamental variability in the optical continuum of symbiotic stars were provided by Boyarchuk *et al.* (1966), Belyakina (1970), Kenyon (1986), Skopal (2001), Skopal (2008) and Jurdana-Šepić & Munari (2010).

Sometimes symbiotic stars experience unpredictable outbursts characterized by  $\sim 1-3$  mag (multiple) brightening(s) in the optical, observed on the timescale of a few months to years/decades (see e.g., historical LCs of FN Sgr, Z And, AX Per of Brandt *et al.*, 2005; Leibowitz & Formigini, 2008; Skopal *et al.*, 2011) with signatures of a mass-outflow (e.g., Fernandez-Castro *et al.*, 1995; Esipov *et al.*, 2000; Skopal, 2006; McKeever *et al.*, 2011; González-Riestra *et al.*, 2013). Outbursts of symbiotic stars are called ‘Z And-type’ outbursts, as they were observed in the past for a prototype of the class of symbiotic stars – Z And (Kenyon, 1986). We name this stage as the *active phase*.

According to the basic composition of symbiotic binaries (see above), modelling the spectral energy distribution confirmed the presence of three basic components of radiation in their spectrum – two stellar from the giant and the hot component and one nebular from the ionized circumbinary environment. Their contributions in the optical rival each other and are different for different objects, and variable due to activity and/or the orbital phase (see Figs. 2–22 of Skopal, 2005). During active phases, the ionization structure of symbiotic binaries changes significantly (e.g. Cariková & Skopal, 2012), which causes dramatic changes of the LC profiles with respect to the wave-like variation during the quiescence. In special cases, transient narrow minima (eclipses) can emerge in the LC for systems with a high orbital inclination (e.g. Belyakina, 1991), whose position and profile is a function of the stage of the activity (Skopal, 1998).

With respect to the above mentioned principal behaviour of symbiotic stars, their LCs bear a great deal of information about the location and physical properties of the radiative sources in the system. Above all, the multicolour photometry represents an important complement to spectroscopic observations and those obtained at other wavelengths. Their monitoring also plays an important role in discoveries of unpredictable outbursts of symbiotic stars.

In this paper, we present results of our long-term monitoring programme of photometric observations of selected symbiotic stars, originally launched by Hric & Skopal (1989). It continues its part XII (Skopal et al., 2007) and XIII (Skopal et al., 2012) by collecting new data obtained during the period from November, 2011 to December 2018. Their acquisition and reduction are introduced in Sect. 2. Sect. 3 describes the most interesting features of the LCs that deserve further investigation. Conclusions are found in Sect. 4.

## 2. Observations and data reduction

Our photometric measurements were carried out at different observatories using different devices and techniques. Multicolour photometric measurements were obtained mostly at the Stará Lesná observatory (pavilions G1 and G2) operated by the Astronomical Institute of the Slovak Academy of Sciences using two 60 cm, f/12.5 Cassegrain telescopes and one 18 cm, f/10 Maksutov-Cassegrain telescope. New observations cover the period between November 2011 and December 2018.

(i) In the pavilion G2, classical photoelectric  $UBV$  observations in the standard Johnson system were obtained by a single-channel photoelectric photometer mounted in the Cassegrain focus of the 60 cm reflector (see Skopal et al., 2004; Vaňko et al., 2014a,b, 2015, in detail). We performed these measurements till February 2016, when they were completely replaced by the observations with CCD detectors. Magnitudes obtained with photoelectric photometer were determined using the comparison stars listed in Table 1 of Skopal et al. (2012). Maximum internal uncertainty of these night-means (rms) is of a few times 0.01 in the  $B$ ,  $V$  filters and up to  $\sim 0.05$  mag in the  $U$  passband.

(ii) CCD photometric measurements were obtained in the standard Johnson-Cousins  $UBVR_CI_C$  system, using three different CCD cameras. Until January 2016, one of the 60 cm telescope was equipped with Moravian Instruments G4-9000 CCD camera ( $3056 \times 3056$  px, pixel size:  $12\mu\text{m} \times 12\mu\text{m}$ ), for  $BVR_CI_C$  photometry. Currently, we are using the FLI ML3041 CCD camera ( $2048 \times 2048$  px, pixel size:  $15\mu\text{m} \times 15\mu\text{m}$ , scale: 0.4 arcsec/px, FoV:  $14' \times 14'$ ) mounted at the 60 cm telescope in the G2 pavilion to measure  $UBVR_CI_C$  magnitudes, and the SBIG ST10 MXE CCD camera ( $2184 \times 1472$  px, pixel size:  $6.8\mu\text{m} \times 6.8\mu\text{m}$ ) in the Cassegrain focus of the 18 cm telescope in the G1 pavilion for  $BVR_CI_C$  photometric observations. As the 18 cm telescope is fixed with the 60 cm one for the mid-resolution ( $R \sim 11000$ ) echelle spectroscopy, it is also used to obtain simultaneous photometry for absolute flux calibration of the spectroscopic observations.

Standard reduction of the CCD images was done using the IRAF-package software<sup>3</sup>. The corresponding magnitudes were obtained with the aid of the

---

<sup>3</sup>IRAF is written and supported by the National Optical Astronomy Observatories (NOAO) in Tucson, Arizona

**Table 1.** Magnitudes of comparison stars used for our targets. The denotation of the stars is adapted from Henden & Munari (2006), if not specified otherwise.

Star	$V$	$B$	$U - B$	$V - R_C$	$R_C - I_C$
Comparison stars in the field of EG And					
a	8.574	10.114	1.965	0.819	0.759
b	10.118	11.145	0.822	0.539	0.495
Comparison stars in the field of Z And					
$\beta$	9.044	9.474	0.095	0.292	0.202
$\gamma$	9.229	10.549	1.229	0.744	0.681
a	12.748	13.525	0.375	0.437	0.402
b	14.205	14.765	0.054	0.337	0.352
c	14.083	15.200	0.874	0.624	0.583
d	14.913	15.791	0.293	0.488	0.473
Comparison stars in the field of BF Cyg					
a	11.159	11.449	0.091	0.173	0.208
b	12.417	12.708	0.182	0.155	0.173
Comparison stars in the field of CH Cyg					
b	9.475	10.021	0.079	0.349	0.293
d	10.227	11.288	0.810	0.564	0.453
e	10.852	12.260	1.693	0.790	0.637
f	12.044	12.679	0.183	0.381	0.332
Comparison stars in the field of CI Cyg					
a	8.831	9.445	-0.166	0.425	0.269
b	11.722	11.996	0.198	0.159	0.173
c	12.353	13.170	0.073	0.376	0.368
Comparison stars in the field of V1016 Cyg					
a	12.314	12.866	0.085	0.334	0.315
b	12.887	13.292	0.223	0.237	0.263
Comparison star in the field of V1329 Cyg					
b	12.092	13.445	1.285	0.724	0.646
Comparison stars in the field of AG Dra					
a	10.459	11.018	0.015	0.333	-
b	11.124	11.857	0.183	0.416	0.330
c	11.699	12.244	-0.042	0.335	0.294
d	11.312	12.594	1.135	0.692	0.580
f	13.221	13.707	0.045	0.321	0.257
Comparison stars in the field of Draco C1 <sup>a</sup>					
4	15.363	16.328	0.620	0.517	0.481
7	17.447	18.238	0.298	0.465	0.430
9	17.974	18.981	0.309	0.585	0.581
11	19.339	20.123	0.114	0.445	0.569
12	19.787	20.587	-	0.407	0.643

**Table 1.** continued

Star	$V$	$B$	$U-B$	$V-R_C$	$V-I_C$
Comparison stars in the field of RS Oph					
$\alpha$	9.307	10.543	0.880	0.706	0.650
$\beta$	11.494	12.198	0.160	0.450	0.379
a	13.255	14.272	0.377	0.660	0.652
Comparison stars in the field of AG Peg					
a	10.428	11.059	0.178	0.374	0.308
b	10.672	11.505	0.528	0.508	0.430
c	11.204	11.708	-0.030	0.330	0.302
d	11.650	12.628	0.715	0.537	0.503
Comparison stars in the field of AX Per					
$\alpha$	10.201	10.290	-0.177	0.023	0.043
$\beta$	11.156	12.323	0.993	0.608	0.531
a	12.212	12.854	0.166	0.384	0.366
b	13.012	13.025	-0.448	0.004	0.057
c	12.124	13.141	0.700	0.544	0.515
Comparison stars in the field of HBHA 1704-05 <sup>b</sup>					
120	12.627(30)	12.525(10)	11.936(5)	11.581(10)	11.239(10)
123	13.020(30)	12.873(10)	12.260(5)	11.903(10)	11.549(10)
C	11.981(40)	11.357(10)	10.519(5)	10.039(10)	9.626(10)

**Notes:** <sup>a</sup> according to Henden & Munari (2000);

<sup>b</sup> C = TYC 1620-2479 ( $\alpha_{2000} = 19^{\text{h}}54^{\text{m}}55^{\text{s}}$ ,  $\delta_{2000} = +17^{\circ}23'36''$ , Sect. 3.16).

comparison stars of Henden & Munari (2006), listed in Table 1. Each value represents the average of individual measurements during a night. For the conversion of the observed magnitudes to the standard  $UBVR_CI_C$  system, we used transformation coefficients determined from photometric measurements of M67 star cluster. We re-measure the system once a year, but also after each change of instrumentation including coating the mirrors.

(iii) From 2016.9, some multicolour  $BVR_CI_C$  photometry was performed at the private observatory in Liptovská Štiavnica by one of us (M.V.) using the 35 cm, f/4.5 Newtonian reflector equipped with Moravian Instruments G2-1600 CCD camera (CCD chip: KAF 1603ME,  $1536 \times 1024$  px, pixel size:  $9 \times 9 \mu\text{m}$ ). The CCD images were reduced with the MuniWin-package software<sup>4</sup>. Resulting magnitudes agree with the values from G1/G2 stations (see point (ii)) within the errors, which are in the range of 0.02 – 0.03 mag in the  $BVR_CI_C$  filters. Because the camera has only a weak and unevenly sensitivity in the  $U$  passband, we present  $U$  magnitudes only of those symbiotic stars, for which agreement with our data is within  $\pm 0.05$  mag.

<sup>4</sup><http://c-munipack.sourceforge.net/>

(iv) Additional  $UBVR_CI_C$  observations were performed using the 50/70/172 cm Schmidt telescope of the National Astronomical Observatory Rozhen, Bulgaria. A CCD camera FLI PL16803 with the chip size  $4096 \times 4096$  px,  $73.80 \times 73.80$  arcmin field and the scale 1.08 arcsec/px was used. Some observations were also carried out with the VersArray 1300 B CCD camera ( $1340 \times 1300$  px, pixel size:  $20 \mu\text{m} \times 20 \mu\text{m}$ , scale: 0.258 arcsec/px) on the 2 m and 1.3 m telescopes.

Maximum internal uncertainties of our CCD measurements were in most cases comparable to those determined for the photoelectric  $UBV$  photometry (see the point (i) above). In the  $R_C$  and  $I_C$  passband the night-means (rms) errors were  $\lesssim 0.05$  mag. However, in most cases the errors are given in tables (see on-line data).

(v) The photographic magnitudes of FG Ser and HBHA 1704-05 were determined using the digitized plates from the archive of the Sternberg Astronomical Institute of the Moscow University (SAI). The plates were obtained with the 40 cm astrograph at the SAI Crimean Observatory. To extract the LC of these objects, we reprocessed the original scans using the latest version of the VaST-package software<sup>5</sup> featuring the improved photographic aperture photometry calibration technique (Bacher et al., 2005; Sokolovsky et al., 2016).

(vi) In addition, visual magnitude estimates of symbiotic stars AE Ara and AR Pav were performed at the Tetoora Observatory in Australia (R.S.) with the 55 cm, f/3.8 Dobsonian telescope, from 2010. Between 2007 and 2010, estimates of these stars were carried out by Albert Jones<sup>6</sup> at the Carter Observatory, Wellington 1, New Zealand, using his private 32 cm, f/5 reflector. Comparing visual estimates with independently obtained  $V$  magnitudes (e.g., from ASASSN survey), we determined their uncertainties to  $\sim 0.3$  mag for AE Ara (see Figs. 7 and 6 here, and Fig. 3 of Skopal et al. (2007)). For AR Pav we found uncertainties to be even smaller, being of  $\sim 0.2$  mag (Fig. 23 here and Figs. 1 and 10 in Skopal et al. (2001a) and Skopal et al. (2007)).

Tables with data for individual objects are only available on-line at <http://www.astro.sk/caosp/Eedition/FullTexts/vol49no1/pp19-66.dat/>.

### 3. Light curves of the measured objects

#### 3.1. EG And

EG And is one of the brightest symbiotic stars. To date, no outburst was detected during its observational history (Skopal, 1997; Jurdana-Šepić & Munari, 2010, and Fig. 1 here). It is an eclipsing binary consisting of M2.4 III giant and a hot star with a relatively low temperature of 70 000 – 95 000 K in comparison with other symbiotic stars (Oliverson et al., 1985; Kenyon & Fernandez-Castro, 1987; Muerset et al., 1991; Skopal, 2005). The orbital period was most recently

<sup>5</sup><http://scan.sai.msu.ru/vast/>

<sup>6</sup>1920–2013

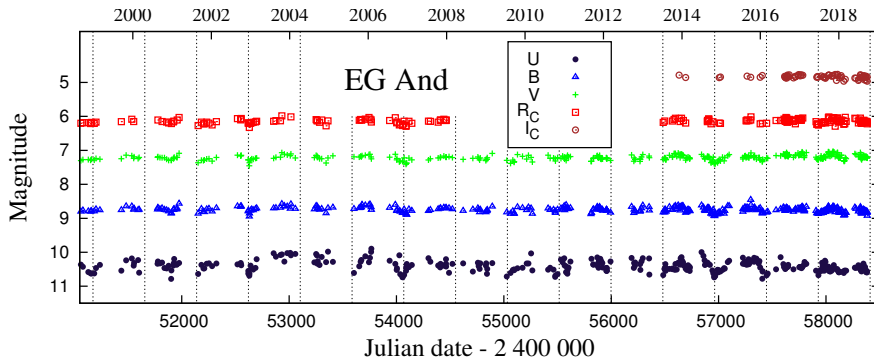


**Figure 1.**  $UBVR_C I_C$  LCs of EG And. Vertical lines represent times of the inferior spectroscopic conjunction of the giant according to the ephemeris of Kenyon & Garcia (2016),  $JD_{\text{sp.conj.}} = 2450208.108(\pm 0.672) + (482.5 \pm 1.3) \times E$ . New observations are displayed with those of Skopal et al. (2012).

determined by Kenyon & Garcia (2016) to  $P_{\text{orb}} = 483.3 \pm 1.6$  days from radial velocities of the cool component derived from echelle spectra observed during more than 20 years. Including their data to all the previously published, they attained an average orbital period of  $P_{\text{orb}} = 482.5 \pm 1.3$  days.

Although EG And persists in a quiescent phase, we can identify a few types of light variability in its LC. Figure 2 shows a double-wave light variation along the orbital motion with minima around times of the spectroscopic conjunctions of the binary components. This variability dominates the light curve of EG And in all passbands. The presence of the secondary minimum around the orbital phase 0.5 in the  $I_C$  filter is confirmed by the long-term photometry in the Johnson's  $I$  filter as published by Percy et al. (2001).

Based on modelling the  $B$  and  $V$  LCs of EG And, Wilson & Vaccaro (1997) attributed the double-wave LC to the tidal distortion of the giant. On the other hand, Skopal (2001) proposed a model, where a partially optically thick, non-symmetrical symbiotic nebula can also generate the observed orbitally-related double-wave light variation by producing different contributions of its emission into the line of sight at different orbital phases. This interpretation does not claim the Roche-filling giant, recently confirmed by Kenyon & Garcia (2016). Finally, we note that Jurdana-Šepić & Munari (2010) didn't find any ellipsoidal variability in their photographic data obtained during 35 years of observations. However, the accuracy of their estimates of 0.1 mag and the presence of additional  $\sim 0.1$  mag variation in  $B$  on the time scale of tens of days (see below) could affect the visibility of the secondary minimum.

The large scatter of data in all filters shown in the phase diagram (Fig. 2) represents real light variations (Skopal, 1997; Skopal et al., 2012). In our data, this variability is best evident in  $B$  and  $V$  after May 2017 ( $\sim JD \sim 2457900$ ,

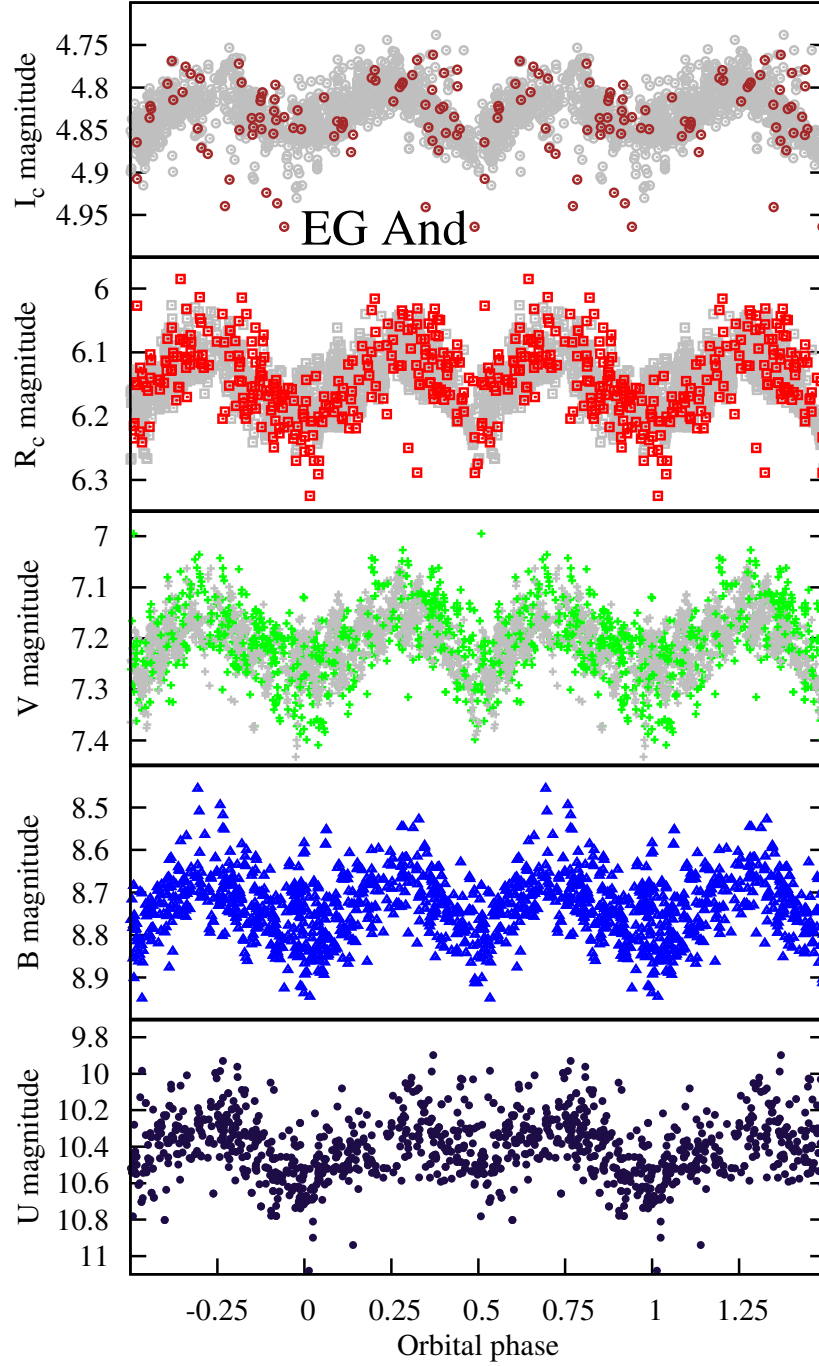


**Figure 2.** Phase diagrams of our  $UBVR_CI_C$  magnitudes for EG And. Compared are  $VRI$  data of Percy et al. (2001) shifted by an appropriate constant (in grey). The large scatter of the data is caused by several types of variabilities (see text).

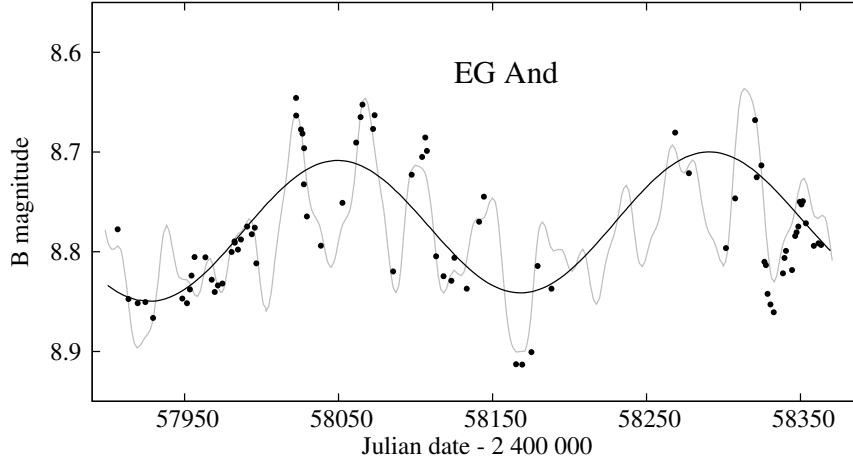


**Figure 3.** A part of the  $B$  LC of EG And, where a light variation with peaks separated by several tens of days is clearly recognized. The grey line represents a model including periods: 241 (half of the  $P_{\text{orb}}$  – black line), 39, 46, and 28 days (see text).

Fig. 3). The peaks are separated by  $\sim 40$  days. Using Fourier analysis on the time interval between May 2017 and March 2018 we identified two periods of  $\sim 39$  and  $\sim 46$  days. Also, the wavelet analysis revealed a period with the highest WWZ statistic of  $\sim 42$  days. Percy et al. (2001) identified a period of 29 days by analyzing the long-term  $VRI$  photometry of EG And. Crowley (2006) suggested, that the period of  $\sim 28$  days with a variation of  $\sim 0.1$  mag is consistent with small radial pulsations of the red giant photosphere. Although we examined only the short time interval, we found a  $\sim 28$  days period in the  $B$  data. When using all our data in  $B$  together with those of Skopal (1997) and Skopal et al. (2012), we identified a period of  $\sim 29$  days. It has, however, lower significance than that of 42 days, which we did not find using all the data. The brightness of the star in  $U$  filter was observed less frequently and these "pulsations" are not so obvious. In our data, we found only a period of  $\sim 27$  days after  $JD \sim 2457900$ . The light curve with  $U$  magnitudes shows more chaotic behaviour, with variation up to  $\sim 0.5$  mag. The observed brightenings could be related to the enhanced mass loss rate from the giant due to pulsations of the giant. The enhanced mass loss from the giant increases the density of the circumstellar matter and hence the accretion rate onto the WD. The enhanced accretion can increase the luminosity of the WD, and thus also the nebular radiation, which dominates the  $U$  passband (Crowley, 2006; Skopal, 2005; Skopal et al., 2012).

Finally, there is probably present a very long-period light variation on the time-scale of several years. It is apparent mainly in the  $U$  brightness, which peaks between the years 1986–1989 (Skopal, 1997) and 2004–2006 (Skopal et al., 2012).

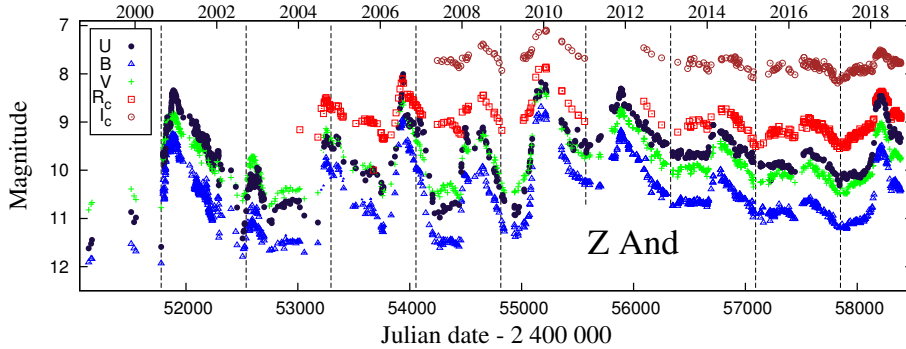


**Figure 4.** As in Fig. 1, but for Z And. Times of the inferior conjunctions of the giant (vertical lines) are according to the ephemeris of Fekel et al. (2000a),  $JD_{\text{sp.conj.}} = 2450260.2(\pm 5.4) + (759.0 \pm 1.9) \times E$ . Data from Skopal et al. (2007, 2012) are supplemented by our data from 2011.9.

This light variation has the highest amplitude in  $U$  ( $\pm 0.1$  mag) and lowest in  $R_C$  and  $I_C$  band ( $\pm 0.025$  mag).

### 3.2. Z And

Z And is considered to be a prototype of the class of symbiotic stars. The binary consists of a late-type M4.5 III red giant and a WD accreting from the giant's wind on the 758-day orbit (e.g. Nussbaumer & Vogel, 1989; Fekel et al., 2000a). The current active phase has begun in September 2000 (Skopal et al., 2000a), being followed with a series of outbursts with the main optical maxima in December 2000, July 2006, December 2009 and December 2011 (see Fig. 4). At/after the 2006 and 2009 maxima, highly collimated bipolar jets were detected as the satellite emission components to  $H\alpha$  and  $H\beta$  lines (Skopal & Pribulla, 2006; Skopal et al., 2018).

Our new photometry is shown in Fig. 4. After the major 2009 outburst, we detected four new main peaks in the LC. The first occurred in November 2011 ( $JD_{\text{Max}} \sim 2455887$ ) with maximum  $U \sim 8.3$  mag). Then the brightness was continuously fading until March 2013 ( $JD_{\text{Min}} \sim 2456353$ ) to  $U \sim 9.7$  mag. The next maximum occurred between February and May 2014 at  $U \sim 9.1$  mag. In June 2016, the star's brightness slightly increased to  $\sim 9.6$  mag, and then declined to the lowest level at  $U \sim 10.3$  mag, in April 2017. In October 2017, Z And started the recent most pronounced outburst since that in 2011. The brightness steeply increased to the maximum of  $U \sim 8.4$  mag in April 2018, following a decrease to the present (December 2018).

The profiles of the observed outbursts since 2011 are very similar. The steep increase of the brightness, followed by a slower decline and separated from the next increase with a standstill in the brightness. In April 2017, we observed a

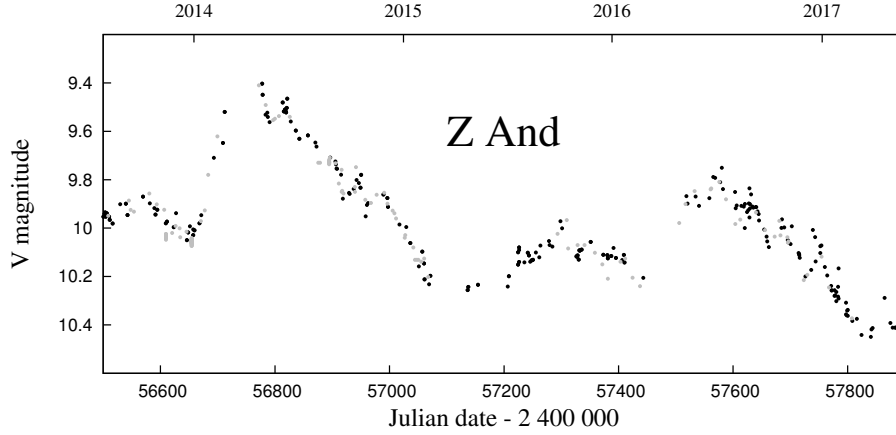


**Figure 5.** The  $V$  LC of Z And from the AAVSO database (grey points) and our measurements (black points). Observations suggest the presence of a 58-d periodic variability.

short decline by  $\sim 0.25$  mag in  $U$  just before the phase of relatively constant brightness, close to the orbital phase  $\varphi \sim 0$ , as observed in the LC of BF Cyg (see Fig. 30). The  $R_C$  and  $I_C$  LCs show a double-wave light variation.

Our data supplement well those from the AAVSO database, whereby we can detect a light variation with the period of  $\sim 58$  days, best visible in the  $V$  LC (Fig. 5).

### 3.3. AE Ara

AE Ara was specified as a symbiotic star on the basis of its infrared colours by Allen & Glass (1974). It is an S-type symbiotic star with the orbital inclination of  $51^\circ$  (Fekel et al., 2010), thus no eclipses are observed in the LC. The orbital period of  $812 \pm 2$  days was determined by Mikołajewska et al. (2003) using the visual photometry during the 1980s and 1990s decades. Using radial velocity measurements from the near-IR spectrum obtained during 2001 – 2009, Fekel et al. (2010) found the value of  $803 \pm 9$  days.

The published photometric data consist mainly of visual estimates. They are in good agreement with photometric  $V$  magnitudes published by Skopal et al. (2007) and  $V$  magnitudes released as a part of the ASAS<sup>7</sup> program (Pojmanski, 2002). According to the LC evolution, AE Ara was in quiescent phase until the beginning of 2006, when the system entered a new active phase (see Fig. 3 of Skopal et al., 2007, and Fig. 6 here).

<sup>7</sup>All Sky Automated Survey

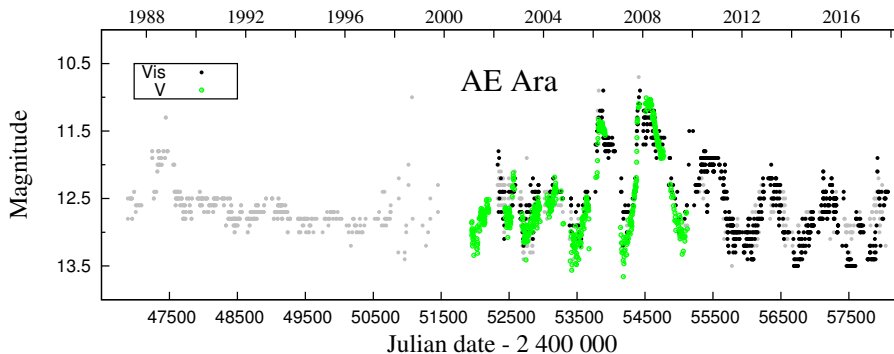


**Figure 6.** The LC of AE Ara consisting of visual estimates from the AAVSO database (grey dots), our data (black) and  $V$  magnitudes from ASAS database (green).

Here we present new visual observations from 2007 (see Sect. 2, point (vi)). Figure 6 shows that AE Ara was in an active phase from 2006 to  $\sim 2014$  with the maximum  $V \sim 11$  mag at the beginning of 2008 that was followed by a gradual decrease throughout a few orbital cycles. Applying the Fourier analysis for the AAVSO<sup>8</sup> data,  $V$  magnitudes from ASAS and our measurements between March 2006 and July 2016, we estimated the orbital period of AE Ara to  $\sim 860$  days (Fig. 7). To confirm this result, we also used a different approach. We fitted the data with a function

$$m(t) = A \times e^{-\gamma t^2} \sin[(t - t_0)2\pi/P] + v_1 t + v_2, \quad (1)$$

where the variation of the magnitude  $m(t)$  with time  $t$  in Julian days is described by a sinus function with the phase shift  $t_0$  and the period  $P$ . In our approach, the decrease of the amplitude  $A$  is given by a damping parameter  $\gamma$  and the star's brightness declines linearly with time, given by parameters  $v_1$  and  $v_2$ . The resulting fit (Fig. 7) yields the period  $P = 850 \pm 20$  days and the 60% decline in the amplitude variations from 2006.2 to 2016.6. During this time, the brightness of the system decreased with a factor of  $\sim 1.4$ . Our analysis suggests that the orbital period indicated during the transition from the active to the quiescent phase (2006.2 – 2016.6) is larger than that determined during the quiescent phase by Mikołajewska *et al.* (2003) and that from radial velocities of Fekel *et al.* (2010).

Analysis of the minima positions in the historical LCs of symbiotic stars revealed apparent changes in their orbital periods that are systematic, depending on the level of activity of symbiotic binary (Skopal, 1998). For example, after the main 1895 outburst of BF Cyg the minima were separated with  $\sim 770$  days along the decrease of the star's brightness, which indicates a longer orbital

<sup>8</sup>American Association of Variable Star Observers

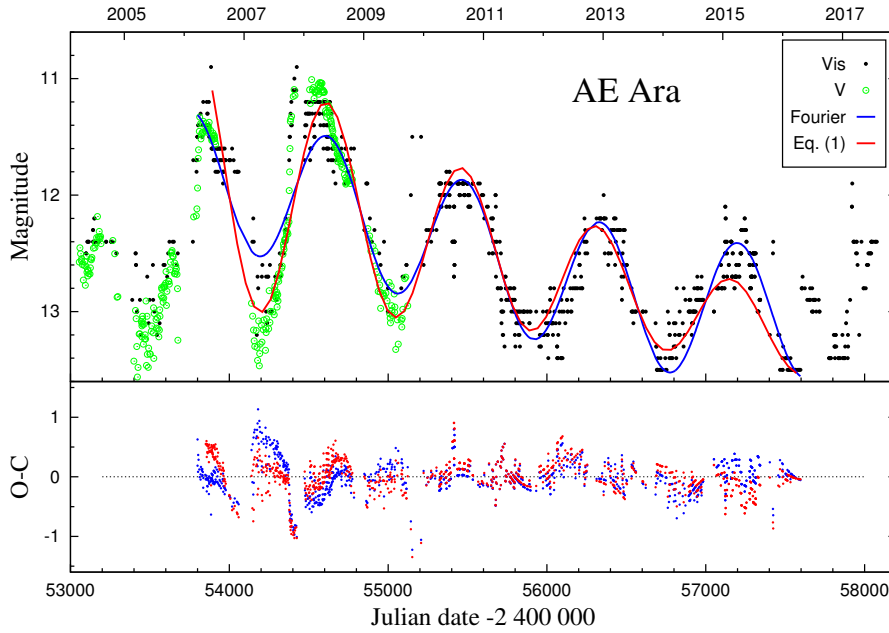


**Figure 7.** Top: Our fits to the  $V$ /visual LC of AE Ara during its transition from the active to quiescent phase (2006.2 – 2016.6). The corresponding orbital period is larger than that determined from the quiescent LC (see text). Bottom:  $O - C$  residuals between the fit from Fourier analysis (blue points), Eq. (1) (red points) and the data.

period than given by the spectroscopic orbit (757.2 days; see Fekel et al., 2001). The nature of the larger apparent orbital period determined for AE Ara during the brightness decline after the 2006 outburst will be probably the same as for BF Cyg. Understanding of this very interesting effect requires a more detailed analysis, which is out of the scope of this paper.

### 3.4. BF Cyg

Observational history of the eclipsing symbiotic star BF Cyg began more than 120 years ago (Jacchia, 1941, and references therein). The main feature of the LC is a very slow decrease in the brightness, from the  $\sim 1894$  nova-like outburst to  $\sim 1985$ , when the brightness in  $B$  decreased by more than 3 mag (see Fig. 1 of Skopal et al., 1997). Simultaneously, periodic or eruptive variations in the star's brightness were observed. The historical LC was analyzed by Leibowitz & Formigini (2006). They identified several periods in the optical LC. Beside the orbital period  $P_{\text{orb}} = 757.3$  days, (Pucinskas, 1970; Fekel et al., 2001), they indicated a 798.8-d period, which they attributed to the rotation of the giant. In

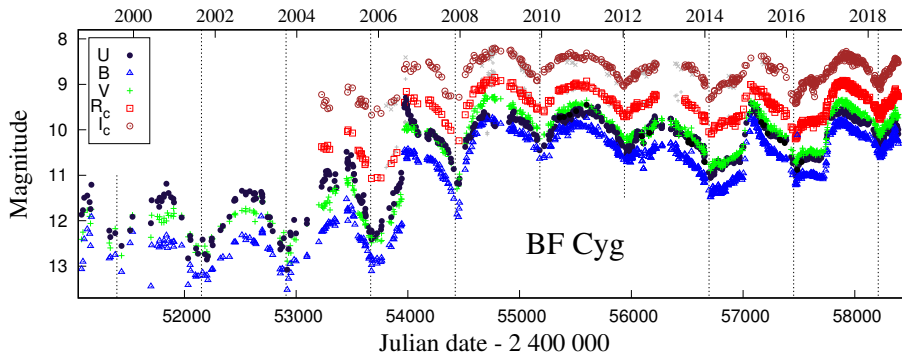


**Figure 8.** As in Fig. 1, but for BF Cyg. Vertical lines represent times for conjunctions with the giant in front according to the ephemeris of Fekel et al. (2001),  $JD_{\text{sp.conj.}} = 2451395.2(\pm 5.6) + (757.2 \pm 3.9) \times E$ . Our new observations are displayed with the data published by Skopal et al. (2007, 2012), Yudin et al. (2005) and, for a comparison, data from the AAVSO database (grey points).

addition, they showed that the most pronounced outbursts repeat every  $\sim 6376$  days, predicting a new outburst for 2007.

A new active phase began around the mid of 2006, reaching the peak in September 2006 (Munari et al., 2006; Iijima, 2006; Skopal et al., 2007; McKeever et al., 2011).

Figure 8 shows the multicolour LCs of BF Cyg from 1999 to our last observations in December 2018. The light variation after the 2006 outburst is modulated by the orbital motion, showing broad minima around the inferior conjunction of the giant (orbital phase  $\varphi = 0$ ), similar to those observed during quiescent phases. After the rapid descent to the eclipse in December 2013, the LC changed in profile. In 2014 and 2016 the minima were followed by a phase of a relatively constant brightness until  $\varphi \sim 0.4$ . It is of interest to note, that similar light variation was observed also in the LC of AX Per and Z And (see Fig. 30). During the 2014 eclipse, BF Cyg reached the lowest brightness since the deep eclipse in 2007. Thereafter, the overall brightness of the system was gradually increasing. The minima in 2014 ( $U \sim 11.0$ ), in 2016 ( $U \sim 11.0$ ) and in 2018 ( $U \sim 10.4$  mag) occurred  $\sim 14$ ,  $\sim 17$  and  $\sim 20$  days after the predicted inferior conjunction of the giant, according to the ephemeris of Fekel et al. (2001). After that we observed a steep increase of the brightness (bursts, see Skopal et al., 2017a, for the 2016/2017 one), which peaked around  $\varphi \sim 0.5$ . A similar profile of the light variation is present in all  $UBVR_CI_C$  filters, although in the  $I_C$  filter it is less evident. After the most recent minimum in 2018 ( $JD_{\text{Min}} \sim 2458230$ ) the brightness of BF Cyg steeply raised to  $U \sim 9.7$  mag at  $JD \sim 2458360$ , but consequently dropped to  $U \sim 10$  mag within  $\sim 30$  days as given by our last measurement.

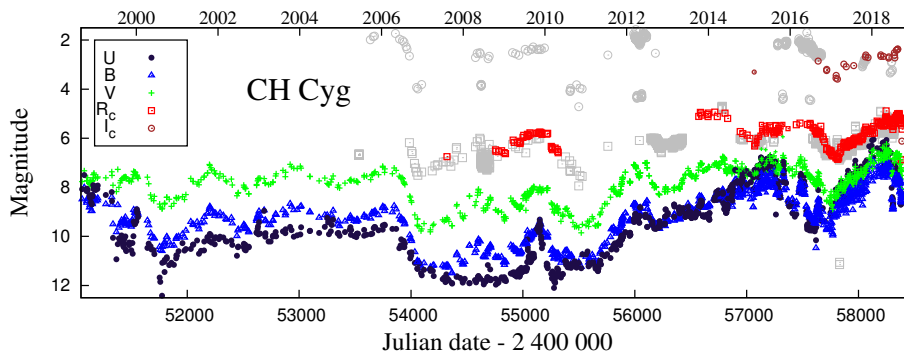


**Figure 9.** As in Fig. 1, but for CH Cyg. New data (from 2011.9) are supplemented with those published by Skopal et al. (2007, 2012) and the AAVSO  $R_C$  magnitudes (grey points).

### 3.5. CH Cyg

The photometric variability of CH Cyg is probably the most intriguing from all well-observed symbiotics. The light variations are observed on very different time-scales, from minutes to decades. It is believed that the rapid light variation (flickering, flares and bursts) and other types of stochastic variability are connected with accretion phenomena in the system. Also possible pulsation of both the cool giant and the hot component, orbital motion(s) in the system of unknown composition (binary or triple star system?) and dust obscuration events make the resulting light and its changes even more complex (e.g. Mikolajewska et al., 1988; Skopal et al., 1996; Iijima, 1998; Motta & Motta, 2000; Corradi et al., 2001; Skopal et al., 2002; Sokoloski & Kenyon, 2003; Bondar' & Prokof'Eva, 2006; Biller et al., 2006; Taranova & Shenavrin, 2007; Bogdanov & Taranova, 2008; Hinkle et al., 2009; Pedretti et al., 2009; Skopal et al., 2010; Karovska et al., 2010; Sokoloski et al., 2010; Shugarov et al., 2012; Stoyanov et al., 2012; Shugarov et al., 2015; Iijima, 2017; Kondratyeva et al., 2017; Mikayilov et al., 2017; Stoyanov et al., 2018).

Our observations are shown in Figs. 9 and 10. After the June-December period in 2006, when the LC showed a 2 mag decline of brightness in all colours (Skopal et al., 2007), CH Cyg began to gradually increase its brightness. In 2009, a burst was detected simultaneously in the X-rays and the optical  $U, B$  passbands (Mukai et al., 2009; Skopal et al., 2010). Similar bursts were later indicated during October 2015, between February and May 2016 and in September 2016. All bursts were comparable in amplitude ( $\Delta U \sim 1.7$  mag; Fig. 10).

From  $\sim 2015$  we measured a  $\gtrsim 3$  years lasting wave with maxima around July-August 2015 ( $U \sim 7$  mag) and March-April 2018 ( $U \sim 6.4$  mag) and the broad minimum at the end of 2016 with  $U \sim 9.7$  mag. Times of minima depend on the colour. The largest difference of  $\sim 190$  days is between the minimum

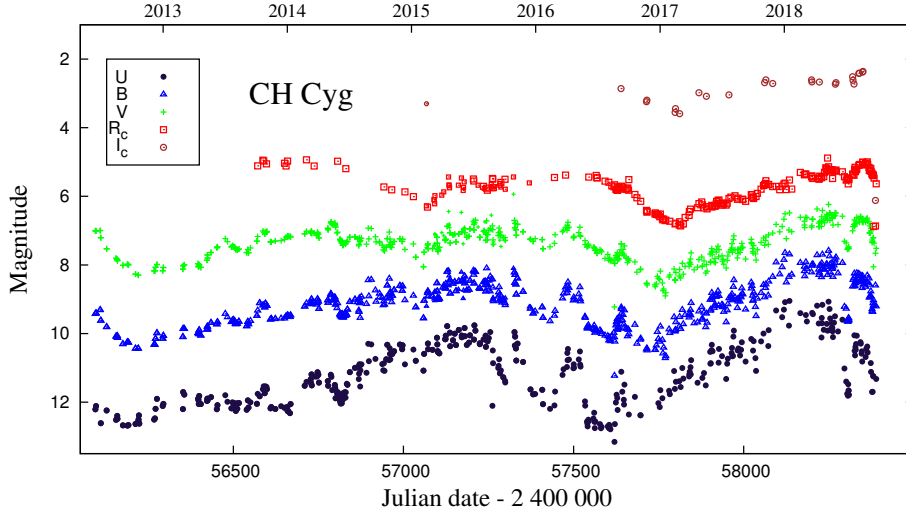


**Figure 10.** Detail of Fig. 9 from 2012.4. The  $U$  and  $B$  LCs were shifted by 3 and 0.7 mag, respectively, for better visualization.

in  $U$  ( $JD \sim 2\,457\,620$ ) and  $R_C$  ( $JD\,2\,457\,814$ ) (Fig. 10), although the  $U$  LC is rather complex during the second half of 2016. It is of interest to note that the 2018 maximum with  $U \sim 6.2$  mag was the highest one after the major 1977-1984 outburst ( $U \sim 5$  mag). The different time of the maximum in  $R_C$  and  $UBV$  filters can be caused by the presence of a  $\sim 95$  day period easily recognized in  $B$ ,  $V$  and  $R_C$  LCs (see Wallerstein *et al.*, 2010). Further, we observed a sharp minimum at  $JD \sim 2\,458\,307$  ( $U \sim 8.8$  mag) and then another decrease by  $\sim 1$  mag until our last observation (see Fig. 10).

### 3.6. CI Cyg

Since September 2008, when CI Cyg underwent its last major outburst, the return to the quiescent phase was interrupted only by two eruptions of lower magnitude (Fig. 11). The first one, disrupted by the eclipse, was described by Skopal *et al.* (2012). The second one with two maxima around  $U = 10.5$  mag was observed during August-September, 2012. Since then, CI Cyg entered a quiescent phase showing the typical brightness variation strongly modulated by the orbital motion in all filters. A secondary minimum around the  $\varphi = 0.6$  was recognizable in the  $BVR_CI_C$  LCs (see Figs. 11 and 12).

According to the basic composition of symbiotic binaries (see Sect. 1), the amplitude of such variability is wavelength dependent with  $\Delta U > \Delta B > \Delta V > \Delta R_C > \Delta I_C$ . Fig. 12 shows that times of the recent wave-like minima are shifted from those predicted by the ephemeris for eclipses. In addition, the shift seems to be a function of the colour. For the 2015 minimum, we deter-

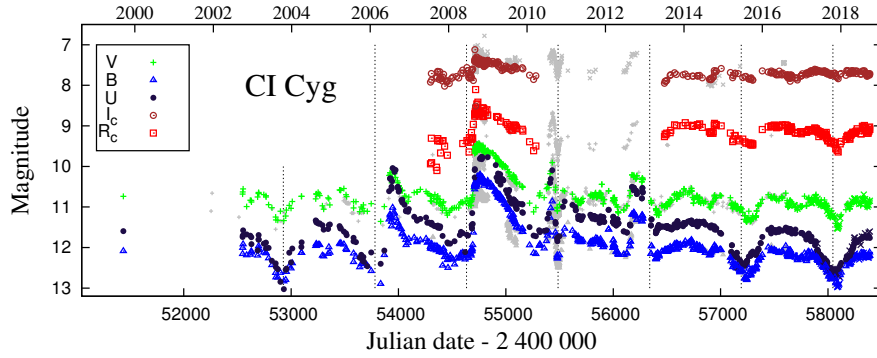


**Figure 11.** As in Fig. 1, but for CI Cyg. The timing of eclipses is given by the ephemeris of Skopal et al. (2012),  $JD_{\text{Ecl.}} = 2441838.8(\pm 1.3) + (852.98 \pm 0.15) \times E$ . Our observations are displayed with those of Skopal et al. (2007, 2012), Siviero et al. (2009) and from AAVSO (grey).

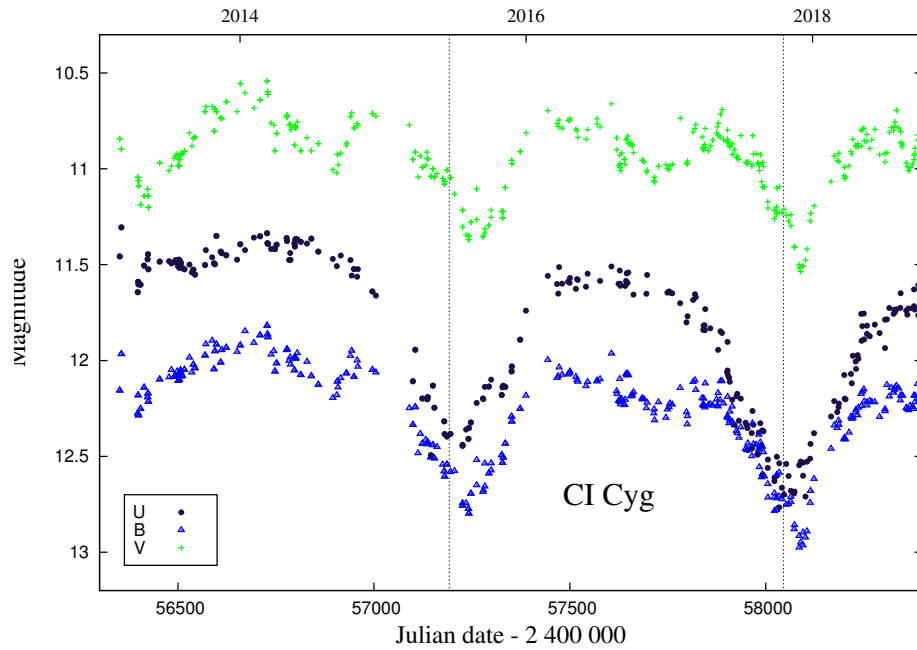


**Figure 12.** During the last two orbital cycles, wave-like orbitally-related variation developed in the LC of CI Cyg – a signature of quiescent phases of symbiotic stars (see Sect. 1). Secondary minima around  $\varphi \sim 0.6$  are indicated in *B* and *V*. In the *V* LC, a variation with a period of  $\sim 73$  days can be found. Vertical lines as in Fig. 11.

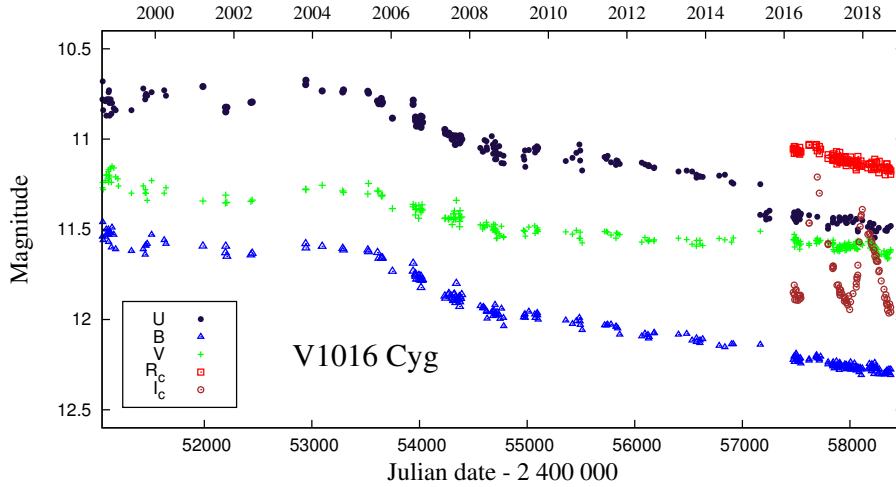


**Figure 13.** As in Fig. 1, but for V1016 Cyg. Here, our new observations are displayed with those published by Parimucha *et al.* (2000) and Arkhipova *et al.* (2008, 2016a,b).

mined the light minima by a simple parabolic fit to  $\text{Min}(B) \sim \text{JD } 2\,457\,237.2$  and  $\text{Min}(V) \sim \text{JD } 2\,457\,253.8$ . For the 2017 minimum, we found its timings at  $\text{Min}(B) \sim \text{JD } 2\,458\,074.4$  and  $\text{Min}(V) \sim \text{JD } 2\,458\,088.4$ . During the last orbital cycle, the LC in all filters is modulated by a light variation with the period of  $\sim 73$  days, which is most pronounced in the  $V$  filter (Fig. 12).

Since 2011 until our last observations, the overall brightness of CI Cyg has been gradually decreasing with a rate of about 0.17 mag per year.

### 3.7. V1016 Cyg

V1016 Cyg underwent a nova-like outburst in 1964 (McCuskey, 1965) when increased its brightness by  $\sim 6$  mag and reached the maximum in 1971. Since then the brightness of the system slowly decreases most of the time. V1016 Cyg is a D-type symbiotic star, with the oxygen-rich cool giant of the Mira-type variable (Harvey, 1974; Schild *et al.*, 1992). Arkhipova *et al.* (2015) refined the pulsation period of the giant to  $P = 465 \pm 5$  days with the minimum at  $JD_{\text{Min}} = (2\,444\,003 \pm 465) \times E$ .

Here, we present  $UBVR_CI_C$  photometric observations of V1016 Cyg obtained after March 2016 (Fig. 13). Pulsations of the giant are clearly apparent in the  $I_C$  filter. The last maximum was observed at  $JD_{\text{Max}} \sim 2\,458\,114$  (Fig. 15). We noticed certain shifts between the data observed in the same passband, but using a different telescope–camera–filter composition (Fig. 14). The shifts are as high as  $\sim 0.15$  mag in  $B$  and  $V$  filter. This is probably caused by the effect usually observed in the LCs of novae during the ‘nebular phase’. The observed flux within a filter is dominated by nebular lines rather than by the underly-

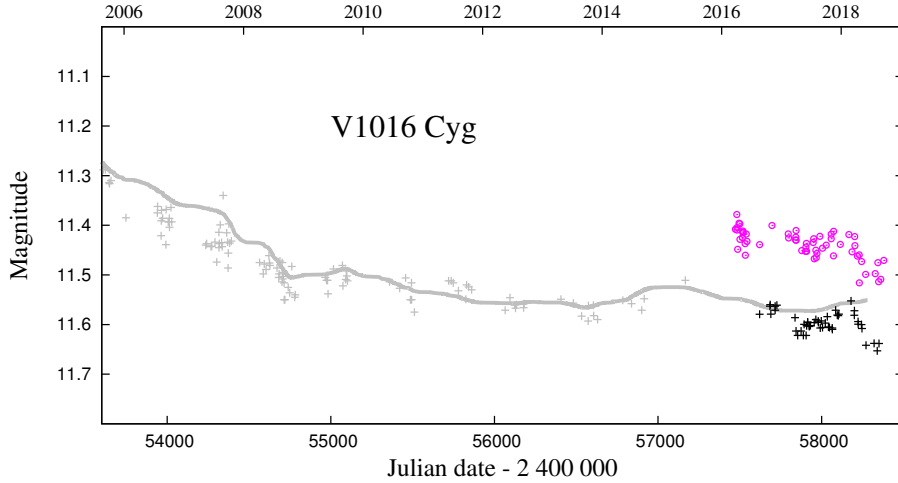


**Figure 14.** The  $V$  LC of V1016 Cyg using different instruments. Gray crosses are data from Arkhipova et al. (2008, 2015, 2016a,b), black crosses are from the private station (M.V.) and G1 pavilion, while the magenta circles are data obtained in the G2 pavilion (see Sect. 2). The grey line represents smoothed LC of visual estimates from the AAVSO database shifted by  $+0.33$  mag.

ing continuum. When using the broadband photometric filters, some prominent emission lines can be located close to the edge of the filter sensitivity. Critical emission lines for this case are  $H\beta$ ,  $O[III]$  4959, 5007 Å,  $H\alpha$  and  $Paa$ , which significantly contribute to the fluxes within  $B$ ,  $V$ ,  $R_C$  and  $I_C$  filters. Hence, a small difference in the response curve of the filter used can result in some shifts in the observed magnitude (e.g. Munari et al., 2015; Arkhipova et al., 2015). Figure 14 demonstrates the effect of strong nebular lines located near to the short-wavelength edge of the  $V$  filter for V1016 Cyg.

In May 2015, Arkhipova et al. (2016a,b) observed a sudden decrease in the  $U$  star's brightness by about 0.17 mag. Our new observations confirm this brightness drop (see Fig. 13). At the same time ( $U - B$ ) and ( $B - V$ ) colours became redder (Fig. 16). This reddening could be partly caused by the variable circumstellar extinction due to the dust produced by the Mira variable and/or by the change of the relative intensity of  $O[III]$  4959 and 5007 Å emission lines, because of their different contribution to the  $B$  and  $V$  magnitude (see Arkhipova et al., 2015). It is of interest to note that the decline in the  $U$  and  $B$  brightness during 2016 occurred around the time of the maximum brightness of the Mira variable for the 465 days pulsation period (at  $JD_{Max} \sim 2\,457\,184$ , see Fig. 15).

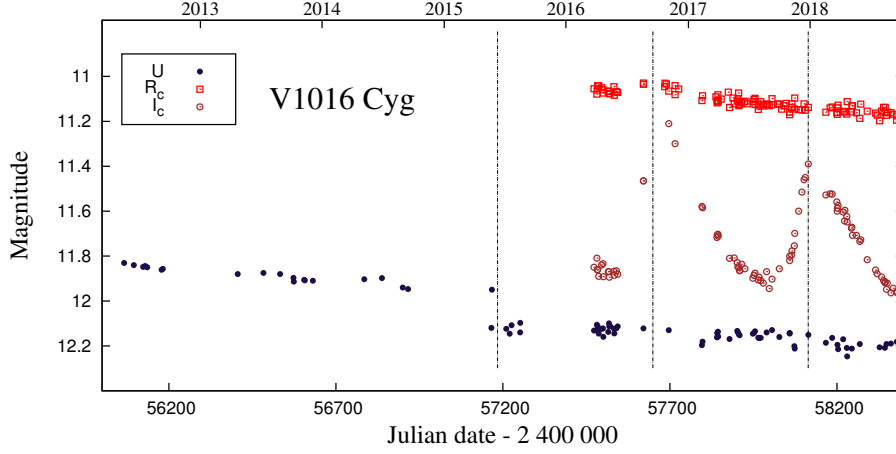


**Figure 15.** A sudden decrease in the  $U$  brightness of V1016 Cyg (around 2015.4) could be connected with pulsations of the Mira variable. The vertical lines correspond to times of the maximum light in the  $I_C$  filter for the period of 465 days. First six points after the decrease are adapted from Fig. 1 of Arkhipova *et al.* (2016a). Their uncertainties are  $<0.01$  mag and  $\pm 10$  days in the scale of magnitudes and JD, respectively.

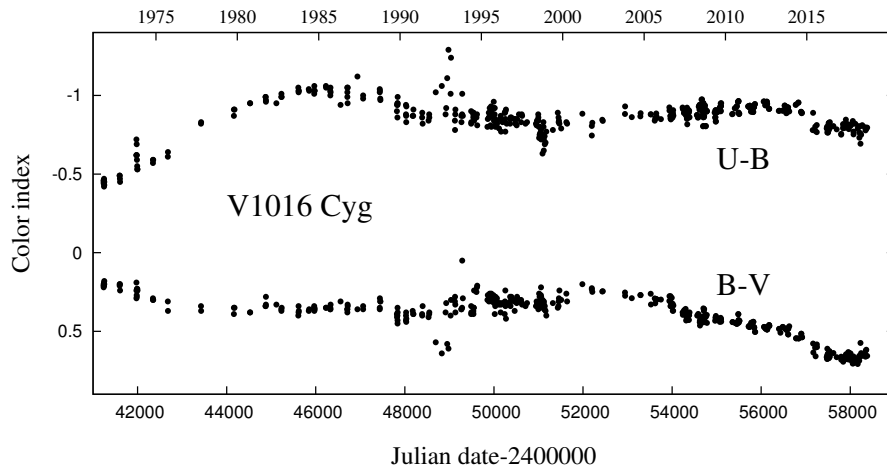


**Figure 16.** Evolution of colour indices of V1016 Cyg. Data sources as in Fig. 13.

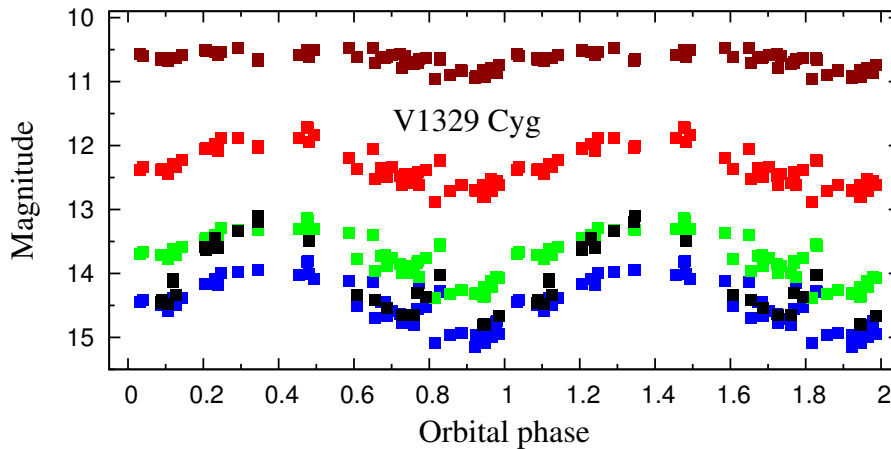


**Figure 17.** Phase diagram of our  $UBVR_CI_C$  magnitudes of V1329 Cyg. We used the ephemeris for the pre-outburst minima (eclipses) as derived by Schild & Schmid (1997),  $JD_{\text{Min}} = 2\,427\,687(\pm 20) + (958.0 \pm 1.8) \times E$ . Denotation of points as in Fig. 1.

### 3.8. V1329 Cyg

V1329 Cyg was originally an inactive star of about 15 mag displaying  $\sim 2$  mag deep eclipses (Stienon et al., 1974; Schild & Schmid, 1997). In 1964, V1329 Cyg underwent a nova-like eruption when brightened by  $\Delta m_{\text{pg}} \sim 3$  mag, peaked around 1968 at  $B \sim 12.0$  mag and developed a wave-like orbitally-related variation in its LC (Kohoutek, 1969; Arhipova & Mandel, 1973; Grygar et al., 1979). This type of photometric variability – characteristic for symbiotic binaries during quiescent phases – dominates the LC of V1329 Cyg to the present (e.g. Skopal et al., 2012, and references therein).

Our new observations of V1329 Cyg are shown in Fig. 17, where they are folded as a function of the orbital phase using the ephemeris of the pre-outburst eclipses derived by Schild & Schmid (1997). The data cover the period from November 19, 2009, to December 25, 2017, i.e.  $\sim 3.1$  orbits. Our measurements confirmed the presence of the orbitally-related light variability with a decreasing amplitude to longer wavelengths:  $\Delta U \sim 1.6$ ,  $\Delta B \sim 1.1$ ,  $\Delta V \sim 0.9$ ,  $\Delta R_C \sim 0.7$  and  $\Delta I_C \sim 0.4$  mag. Such dependence is the result of the superposition of the variable contribution from the nebula and a constant light from the red giant, whose contribution increases to longer wavelengths. Figure 17 also shows that the light minimum precedes the inferior conjunction of the giant by  $\sim 0.1 \times P_{\text{orb}}$ . This effect is caused by a prolate structure of the symbiotic nebula, whose optically thick part is asymmetrically located with respect to the binary axis during quiescent phases of symbiotic stars (see Skopal, 1998, in detail).

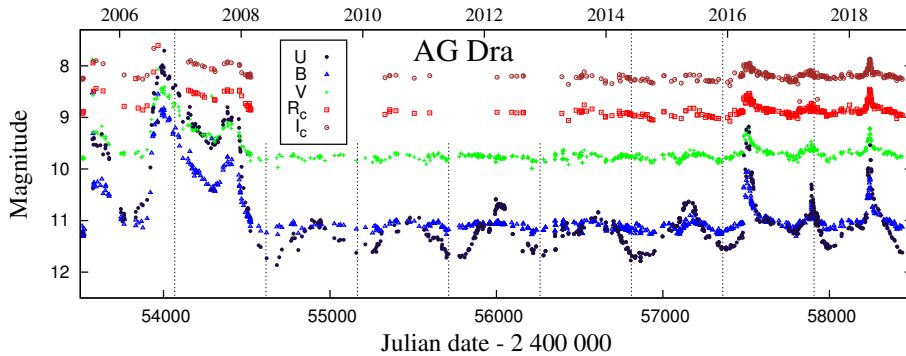


**Figure 18.** As in Fig. 1, but for AG Dra. Vertical lines represent inferior conjunctions of the giant according to the ephemeris of Fekel et al. (2000a),  $JD_{\text{sp.conj.}} = 2450775.3(\pm 4.1) + (548.65 \pm 0.97) \times E$ . Our new observations are displayed with the data published by Skopal et al. (2012) and Munari et al. (2009b).

### 3.9. AG Dra

AG Draconis is a well studied bright symbiotic star. It is a yellow symbiotic binary comprising a K2 III giant (Mürset & Schmid, 1999) and a WD accreting from the giant’s wind on a 549-day orbit (Fekel et al., 2000a). There are no signs of eclipses neither in the optical nor far-UV. Based on spectropolarimetric observations, Schmid & Schild (1997) derived the orbital inclination  $i = 60^\circ \pm 8^\circ.2$ . The system undergoes occasional eruptions, lasting about 1-2 orbital cycles. The stars brightness abruptly increases ( $\Delta U \sim 2$ ,  $\Delta V \sim 1$  mag) showing multiple maxima separated approximately by 400 days, while during quiescent phase the LC shows typical wave-like orbitally-related modulation (e.g. Meinunger, 1979; Skopal, 1998; Hric et al., 2014; Leedjäv et al., 2016, and references therein) The historical LC was analyzed by Formigini & Leibowitz (2012). They confirmed the  $\sim 550$  days orbital period and  $\sim 355$ -day pulsation period of the K-type giant, originally proposed by Gális et al. (1999). Moreover, they reported also  $\sim 373$  days cycle between the outbursts and suggested  $\sim 1160$ -day rotation period of the giant.

González-Riestra et al. (1999) identified cool and hot outbursts differing in their Zanstra temperatures and the LC profile. The former are more pronounced ( $\Delta U \sim 3$  mag) lasting for 1–2 years, while the latter are weaker ( $\Delta U \sim 1$ –2 mag), single brightenings lasting for weeks to months. The last cool outburst was observed during 2006–2007. The following quiescent phase was interrupted with two small brightenings in March 2012 and May 2015 ( $U \sim 10.6$  mag; see Fig. 18). Further, three bright bursts were observed in April 2016 ( $U \sim 9.1$  mag), in May 2017 ( $U \sim 10.3$  mag) and in May 2018 ( $U \sim 9.5$  mag). A multi-peaked profile is apparent especially during the 2016 outburst, where it can be recognized in  $UBVR_C$  filters (Fig. 19).

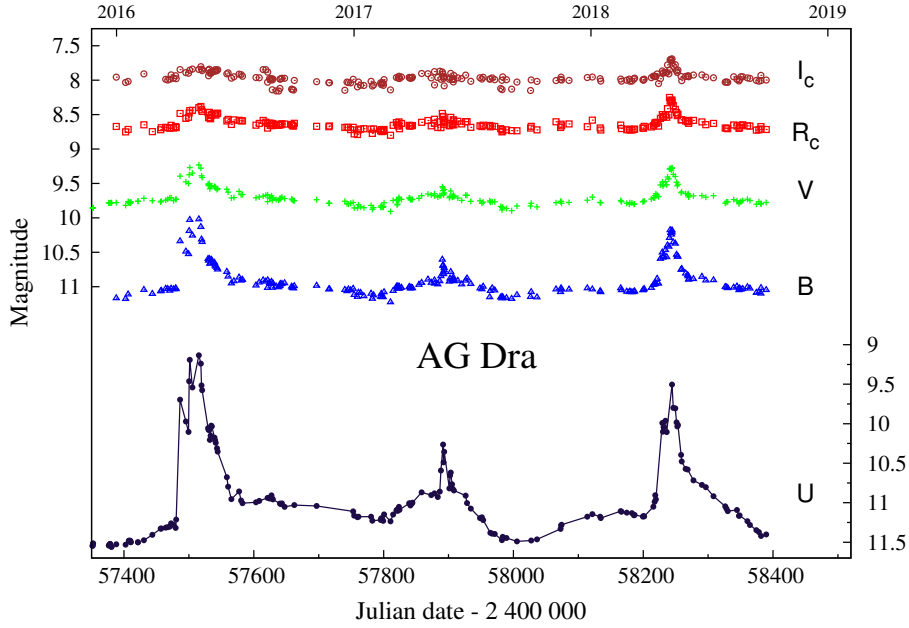


**Figure 19.** Recent three outbursts of AG Dra. Note the multi-peaked structure for the 2016 one.

It is of interest to note that the  $(U - B)$  colour practically did not change during the last 2007 major outburst (see Fig. 20). The plateau part of the LC occurred just between its two maxima. However, the LC profile of the  $(B - V)$  index resembles that of individual LCs. This plateau was not so evident during the 1994 major outburst, while that during the 1981-82 outburst was better comparable with the recent one. The plateau phases during major outbursts of AG Dra are probably caused by a strong dominance of the nebular radiation within the  $U$  and  $B$  passbands (e.g. Skopal, 2005). Then the star's brightness decline here is given by that in the nebular emission, which results in more or less constant value of the  $(U - B)$  index. However, the brightness decrease in, e.g.,  $V$  filter is slower than in a bluer one, because of a significant contribution from the giant in  $V$ , and thus the  $B - V$  index is more similar to individual LC profile (see Fig. 20).

### 3.10. Draco C1

The symbiotic star Draco C1 is located in the Draco dwarf spheroidal galaxy (DdSg). Its symbiotic nature was discovered by Aaronson et al. (1982) within a grating prism survey of the DdSg. The spectrum was characterized by strong emission lines superposed on a carbon star continuum. Draco C1 has been stud-

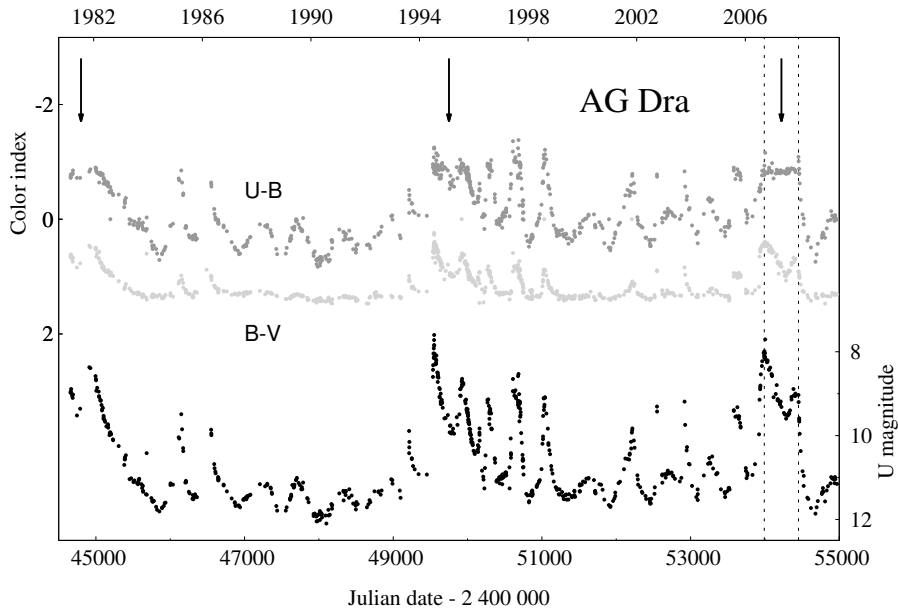


**Figure 20.** The  $(U - B)$  colour shows a plateau during the cool 2006-07 outburst of AG Dra. Vertical lines bounds its duration. Also during previous major outbursts (1981-82, 1994-95) the index was relatively stable (arrows).

ied photometrically for a long time (Munari, 1991; Skopal et al., 2007; Kinemuchi et al., 2008; Henden & Munari, 2008; Munari et al., 2008; Skopal et al., 2012). Long-term photometry showed a variable LC with  $\Delta V \sim 0.1$  mag and periodicity around one year, which could be attributed to the orbitally-related variation of quiescent symbiotic stars.

Our new  $BVR_CI_C$  measurements of Draco C1 cover the period between November 6, 2010, and August 6, 2016.

### 3.11. RS Oph

RS Oph is a symbiotic recurrent nova with the orbital period  $P_{\text{orb}} = 453.6 \pm 0.4$  days (Brandi et al., 2009). To the present, six eruptions were recorded in 1898, 1933, 1958, 1967, 1985 and the last one in 2006. Additional two outbursts probably happened in 1907 and 1954. For the former, only a post-eruption dip was observed on archival photographic plates, because of the season gap in observations (Schaefer, 2004). Similarly, the latter was suggested by Oppenheimer & Mattei (1993) according to the presence of such the dip and the fading tail from the eruption, later confirmed by Adamakis et al. (2011). The mean time between the eruptions is  $\sim 15$  years. After the 2006 outburst, RS Oph remains

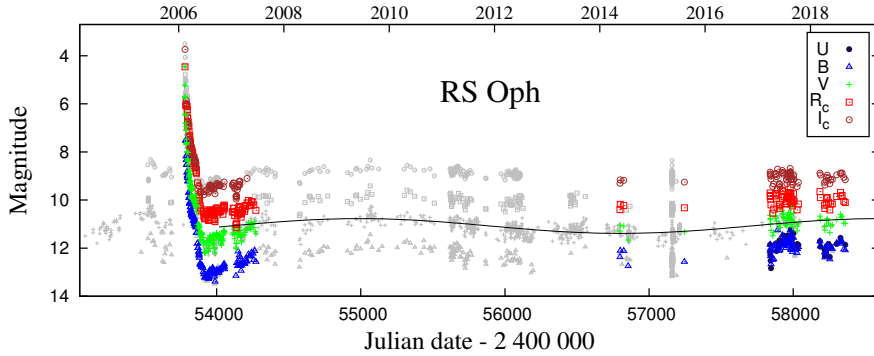


**Figure 21.** As in Fig. 1, but for RS Oph. Our new observations are displayed with the data of Hachisu et al. (2008) (2006 outburst) and from the AAVSO database (grey). The solid line represents a sine function with amplitude  $\Delta V \sim 0.3$  mag and a period of  $\sim 9.4$  years.

in a quiescent phase, during which the LC shows a sine-like variation with the amplitude  $\Delta V \sim 0.3$  mag and a period of  $\sim 9.4$  years (Fig. 21). A large scatter of the data is caused by the presence of flickering with the amplitude of several tenths of a magnitude (e.g. Bruch, 1986; Worters et al., 2007; Zamanov et al., 2015). Our measurements of the rapid light variability of RS Oph are showed in Fig. 22. It is observed in all  $UBVR_C I_C$  filters having the amplitude decreasing with increasing wavelength, because of increasing constant contribution from the giant in longer wavelengths.

### 3.12. AR Pav

AR Pav is eclipsing symbiotic binary with the orbital period of 605 days (Mayall & Shapley, 1937). It consists of an M5 III giant with a mass of  $\sim 2 M_{\odot}$  (Mürset & Schmid, 1999). According to the observed variations in the UV/optical continuum (e.g. Schild et al., 2001; Skopal et al., 2000b), the hot component is highly variable in brightness, size and the geometry as suggested by very different profiles of minima – eclipses (Bruch et al., 1994; Skopal et al., 2000b, 2001a).

Photographic magnitudes of AR Pav were recorded on Harvard chart plates since 1889 (Mayall & Shapley, 1937). Monitoring this star during 1889-1937, the authors classified it as an eclipsing binary of the P Cyg type with an orbital period of 605 days. Comparing consecutive refinements of the orbital period (see Andrews, 1974; Bruch et al., 1994), complemented with new, 1985-1999, observations, Skopal et al. (2000b) found a decreasing trend of the orbital period. The following observations (see Skopal et al., 2001a, 2004) supported this result until the period felt to the value of  $602.8 \pm 0.3$  days as determined from the minima (66), (67) and (68) (Figs. 23 and 24). The period between Min(69) and Min(70), however, raised up to  $607.3 \pm 2.1$  days (Skopal et al., 2007). Authors

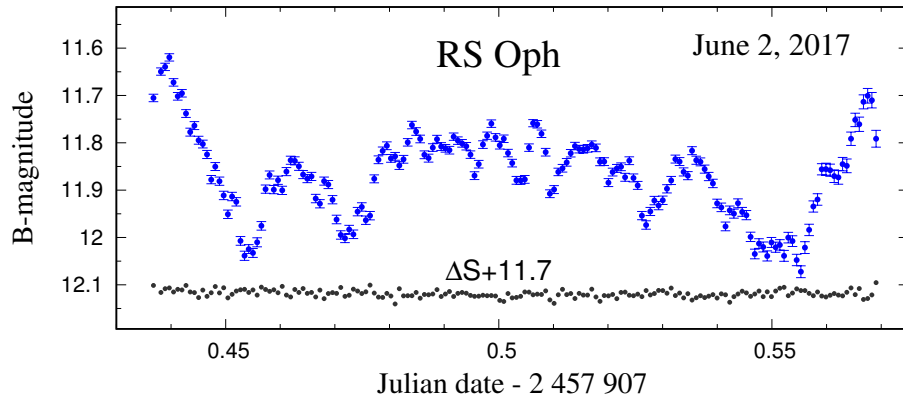
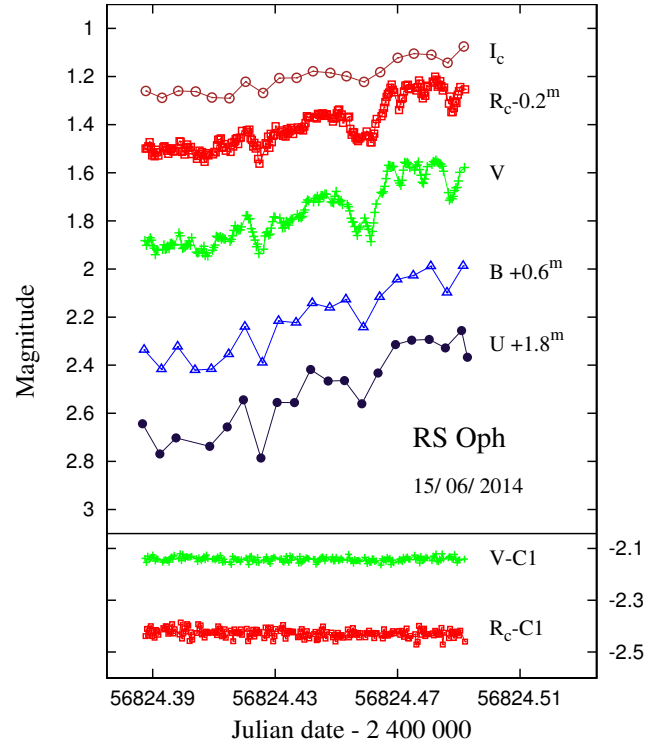


**Figure 22.** Examples of rapid photometric variability of RS Oph. Top panel shows variations in  $UBVR_CI_C$  filters obtained in G2 pavilion (point (ii) of Sect. 2), while the bottom panel shows high-cadence observations in  $B$  acquired at the private station (point (iii) of Sect. 2). Here, we used the star UCAC4-417-071413, ( $V=9.307$  mag,  $B-V=1.236$ ) as the comparison and UCAC4-416-072918 as the check star.  $\Delta S$  denotes their difference in  $B$ .

ascribed this difference to a strongly variable size, geometry and radiation of the eclipsing object, which affects the variation in the minima depth and the overall profile of the eclipse.

**Table 2.** The timing of eclipses in the historical LC of AR Pav

Epoch	$JD_{\text{Min}}$	Ref.*	Epoch	$JD_{\text{Min}}$	Ref.*
4	2413678.4±1.9	1	62	2448742.6±0.6	1
6	14881.3±1.5	1	63	49347.8±0.6	1
9	16705.3±2.3	1	64	49951.8±0.5	1
12	18519.0±3.8	1	65	50555.5±0.8	1
15	20333.4±3.6	1	66	51158.9±0.7	2
21	23960.6±2.0	1	67	51762.8±0.7	2
24	25776.2±3.0	1	68	52364.5±0.7	3
27	27589.5±1.0	1	69	52966.0±2.0	4
47	39679.1±1.7	1	70	53573.3±0.7	4
50	41492.0	1	71	54188.2±4.5	tp
56	45113.7±2.0	1	72	54793.2±1.1	tp
57	45718.7±2.3	1	73	-	-
58	46321.4±2.2	1	74	55989.9±0.6	tp
59	46924.7±0.4	1	75	56599.2±0.3	tp
60	47531.7±0.9	1	76	57205.3±0.9	tp
61	48138.1±0.5	1	77	57807.7±0.8	tp
			78	58409.5±1.0	tp

\* Reference: 1 - Skopal et al. (2000b), 2 - Skopal et al. (2001a), 3 - Skopal et al. (2004), 4 - Skopal et al. (2007), tp - this paper

In this paper, we present our (A.J., R.S.) new visual magnitude estimates, which are in good agreement with photoelectric  $V$  magnitudes (see Skopal et al., 2000b, 2001a, 2004, 2007, and Fig. 23 here). We determined times of new minima between the epoch 71 and 78 using one or several methods (parabolic fit, tracing paper method, Kwee and van Woerden method, sliding integration). Minimum at  $E = 73$  was not determined, because of insufficient data (Fig. 24). Our times of minima (eclipses) together with those published in the literature are listed in Table 2. They correspond to linear ephemeris

$$JD_{\text{Min}} = 2411264.4(\pm 1.7) + (604.47 \pm 0.03) \times E. \quad (2)$$

Residuals between the observed and predicted times of minima (eclipses) are shown in Fig. 25. The  $O - C$  diagram indicates real systematic variation in the minima timing. In general, this can be caused by variable mass transfer and mass accretion resulting in variable size and shape of the eclipsing object, and thus in a variation of times of the light minima.

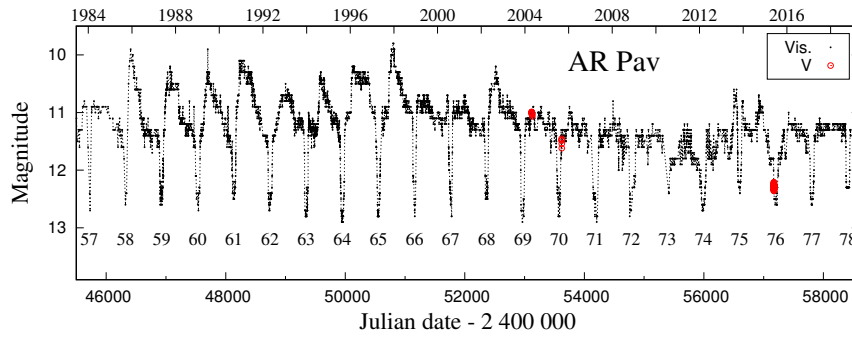


**Figure 23.** The visual LC of AR Pav made by two observers (AJ and RS). Our new observations (see Sect. 2) are displayed with the V data from the AAVSO database (Rolf Carstens) and those published by Skopal *et al.* (2004, 2007).

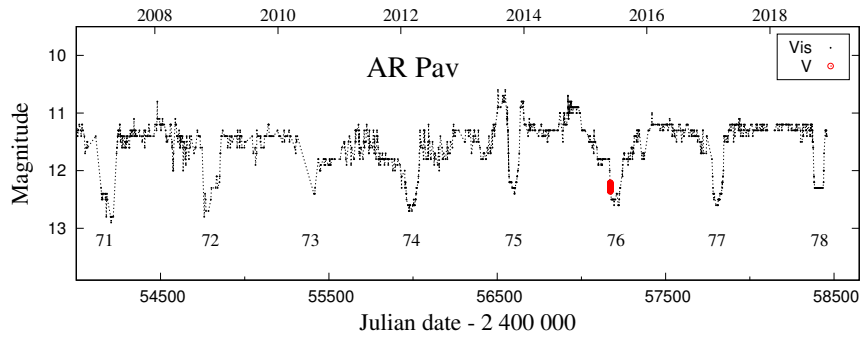


**Figure 24.** The recent low stage of AR Pav between the epoch 71 and 78.

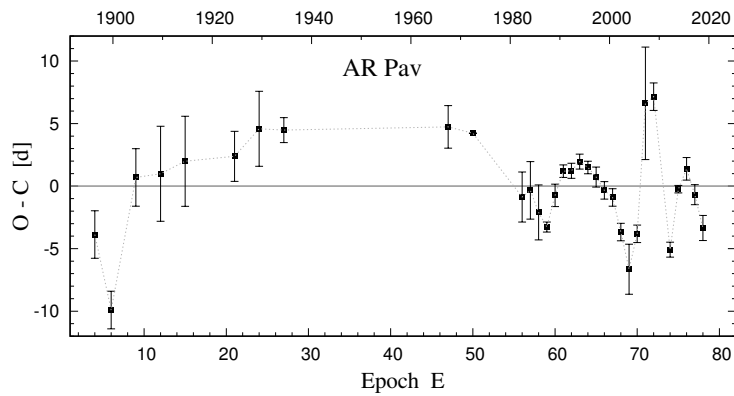


**Figure 25.** O-C diagram for the linear ephemeris (2) determined by timing of eclipses (Table 2) in the historical LC of AR Pav.

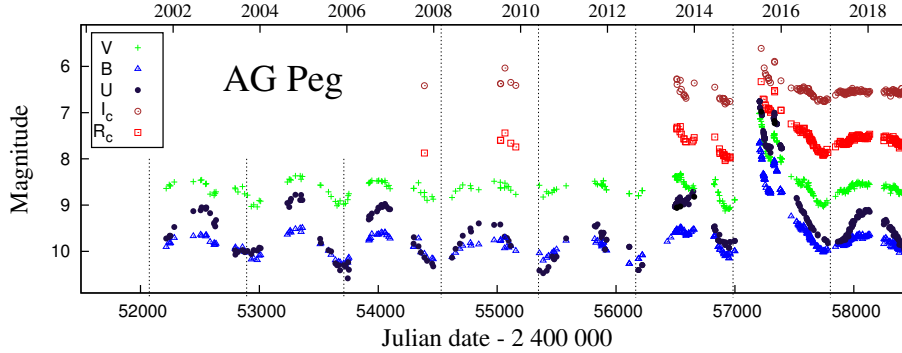


**Figure 26.** As in Fig. 1, but for AG Peg. Data to 2011.9 were published by Skopal et al. (2012). Vertical lines represent inferior conjunctions of the giant according to ephemeris of Fekel et al. (2000b),  $JD_{\text{sp.conj.}} = 2\,447\,165.3(\pm 48) + (818.2 \pm 1.6) \times E$ .

During the higher level of the activity, the LC of AR Pav resembles that of AX Per. However, the maximum light occurs usually around the orbital phase  $\varphi \sim 0.25$  and not during the superior conjunction of the giant (Fig. 30). After 1998, AR Pav reduced its out-of-eclipse activity to only three episodes of the star’s brightening; in 2002, 2013 and 2014 (see Figs. 23 and 24). The flat LC profile between eclipses is observed from  $\sim 2016.5$  to date.

### 3.13. AG Peg

AG Peg is a symbiotic binary comprising a M3 III giant (Kenyon & Fernandez-Castro, 1987) and a WD on an 818-d orbit (e.g. Fekel et al., 2000b). This system is known as the slowest nova ever recorded (Kenyon et al., 1993). Its nova-like outburst began during 1850 (Lundmark, 1921) when it rose in brightness from  $\sim 9$  to a maximum of  $\sim 6$  mag around 1885. Afterwards, AG Peg followed a gradual decline to around 1997 (Boyarchuk, 1967; Kenyon et al., 2001). Then AG Peg entered a quiescent phase with a typical orbitally-related wave-like light variations with the amplitude  $\Delta U \sim 1.4$  mag around the mean of 9.7 mag until June 2015, when erupted again showing a Z And-type outburst (Fig. 26 here, Fig. 1 of Skopal et al., 2017b, and references therein).

The 2015 outburst was first reported by Waagen (2015). According to our multicolour photometry (Fig. 26 here and Fig. 2 of Skopal et al., 2017b), the outburst started around June 5, 2015 ( $JD \sim 2\,457\,177.6 \pm 3.3$ ) at  $B = 9.55 \pm 0.07$  mag and  $V = 8.45 \pm 0.06$  mag, reaching a maximum around June 30, 2015 ( $JD \sim 2\,457\,203.5 \pm 2.0$ ) at  $B = 7.68 \pm 0.05$  mag and  $V = 7.0 \pm 0.1$  mag. After a gradual decline, a sudden re-brightening occurred on October 8, 2015 ( $JD \sim 2\,457\,304.0 \pm 0.5$ ) with a rise in  $U$ ,  $B$  and  $V$  by  $\sim 1$ ,  $\sim 0.7$  and  $0.5$  mag, respectively. In contrast to the first maximum, the secondary one was followed by a plateau phase until November 24, 2015, when the brightness began to decrease gradually.

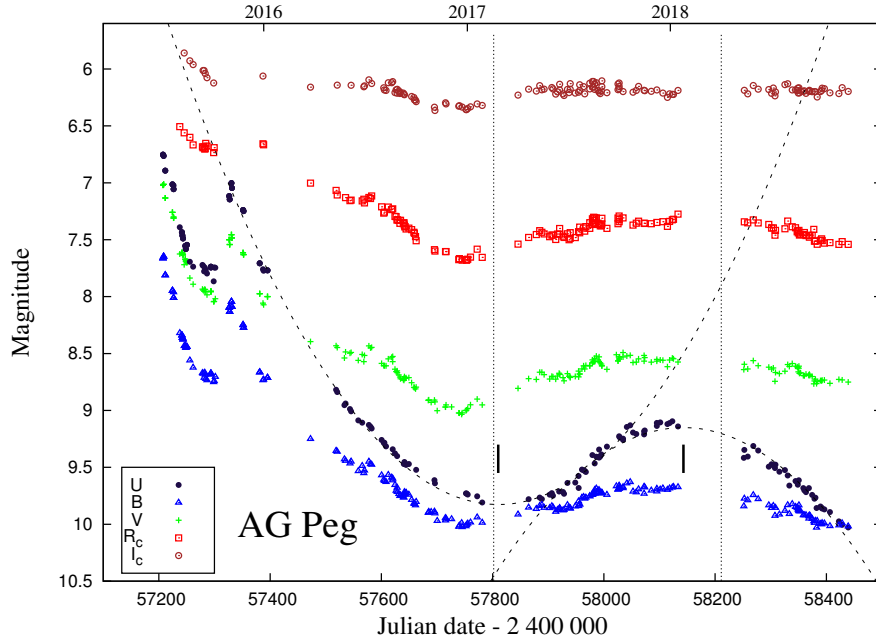


**Figure 27.** Multicolour LCs after the 2015 outburst demonstrating transition of AG Peg to quiescent phase. Dashed curves are quadratic functions, vertical lines represents orbital phase 0 (JD 2 457 801.9) and 0.5 (JD 2 458 211.0) and short vertical bars mark corresponding minimum and maximum in  $U$ .

From August 2016 to the end of our observations (December 2018), the LCs developed a wave, signaling that AG Peg returned to a quiescent phase (see Figs. 26 and 27). The shape of the  $U$  LC could be compared to quadratic functions, which aid us to determine its extrema. The minimum and maximum occurred at  $U \sim 9.8$  and  $\sim 9.1$  at the orbital phase  $\varphi \sim 0.01$  and  $\sim 0.4$ , respectively.

The brightness, the short timescale and the multiple peaks of the 2015 outburst refer to a different type of outburst in comparison with the event in the mid of 19th century. It was shown that the recent outburst was of a Z And-type and that AG Peg obviously entered a new era of its evolution (Tomov *et al.*, 2016; Ramsay *et al.*, 2016; Skopal *et al.*, 2017b).

### 3.14. AX Per

AX Per is an eclipsing binary with the orbital period of  $\sim 680$  days (e.g. Skopal, 1991; Mikolajewska & Kenyon, 1992). The last quiescent phase that lasted from 1995 was interrupted by the  $\Delta U \sim 0.5$  mag flare in July 2007 followed with rapid  $\sim 1$  and  $\sim 0.7$  mag brightenings in  $B$ , during March 2009 and November 2010,

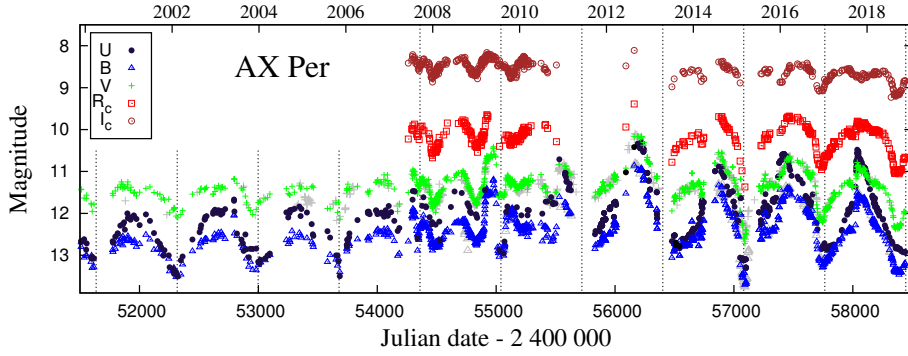


**Figure 28.** As in Fig. 1, but for AX Per. Vertical lines represent the timing of eclipses,  $JD_{\text{Ecl.}} = 2447551.26(\pm 0.3) + (680.83 \pm 0.11) \times E$  (Skopal et al., 2011). New data are complemented with those of Skopal et al. (2011, 2012) and  $V$  from AAVSO (grey).

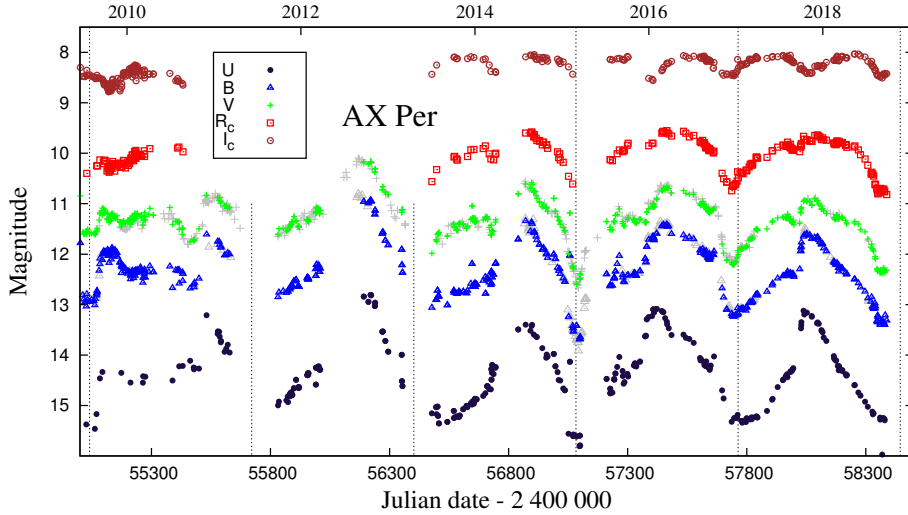


**Figure 29.** The recent evolution of the AX Per LCs covering its current active stage. The  $U$  LC is shifted by +2.5 mag for better visualization.

respectively (Fig. 28), supporting a suggestion of a forthcoming major outburst (Munari et al., 2009a, 2010).

Our new photometric observations cover nearly four orbital cycles during a high level of the star activity. A wave-like profile in all colours with the amplitude of  $\sim 2$  mag are typical for each cycle (Figs. 28 and 29). It is of interest to note that such characteristics can be recognized also in LCs of other active symbiotic binaries. Figure 30 shows a comparison for AX Per, BF Cyg, Z And

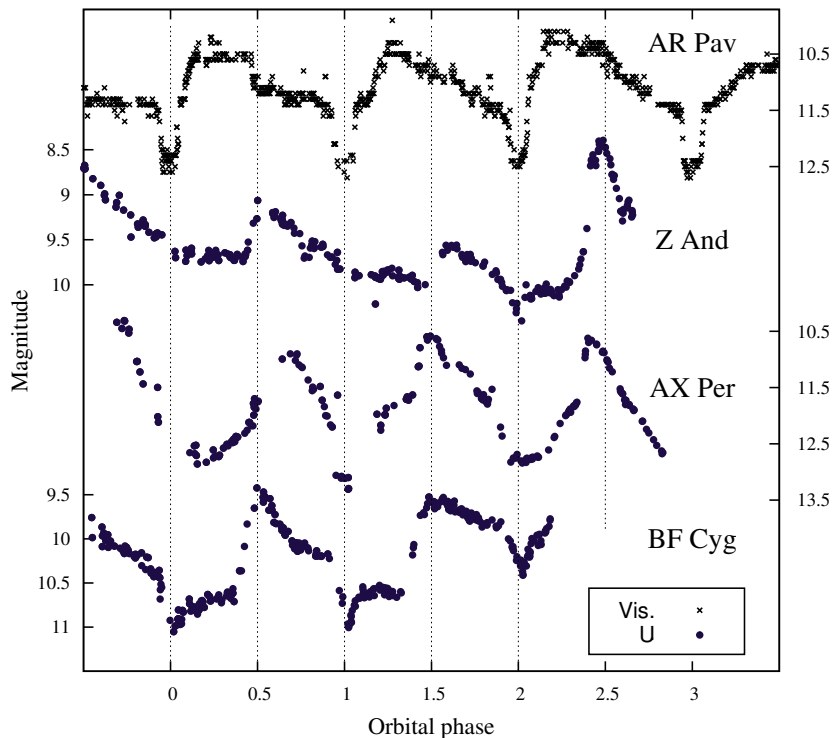


**Figure 30.** Comparison of the recent AX Per LC with those of other active symbiotic stars. The light maximum and minimum usually appear around  $\varphi \sim 0.5$  and  $\sim 0$ , respectively, while the LC of AR Pav shows maxima around  $\varphi \sim 0.25$ .

and AR Pav. The light minimum is always observed around the inferior conjunction of the giant, i.e. at the orbital phase  $\varphi \sim 0$ , and the maximum light around  $\varphi \sim 0.5$ , when the active object is in front.

During the recent active phase, the minima – eclipses differ significantly from those observed during previous active phases (see Fig. 2 of Skopal *et al.*, 2011). For example, the eclipse measured in March 2015 has a narrow, symmetric V-shaped profile in  $B$  and  $V$  with the minimum at  $JD_{\text{Min}} \sim 2457090.8$ , while in  $U$  the LC is rather flat. The following ‘eclipse’ from December 2016 ( $JD_{\text{Min}} \sim 2457743$ ) is much broader and asymmetric in  $B$ ,  $V$  and  $R_C$  and even flatter in  $U$ , lasting from  $\varphi \sim 0.9$  to  $\sim 1.2$  (Fig. 29). We note here that a very similar eclipse profile was observed between 1958 and 1972 (Fig. 31), when AX Per was in quiescent phase (Myalkovskij, 1977; Skopal *et al.*, 2001b). According to  $V$ ,  $R_C$  and  $I_C$  LCs, the last observed minimum started in August

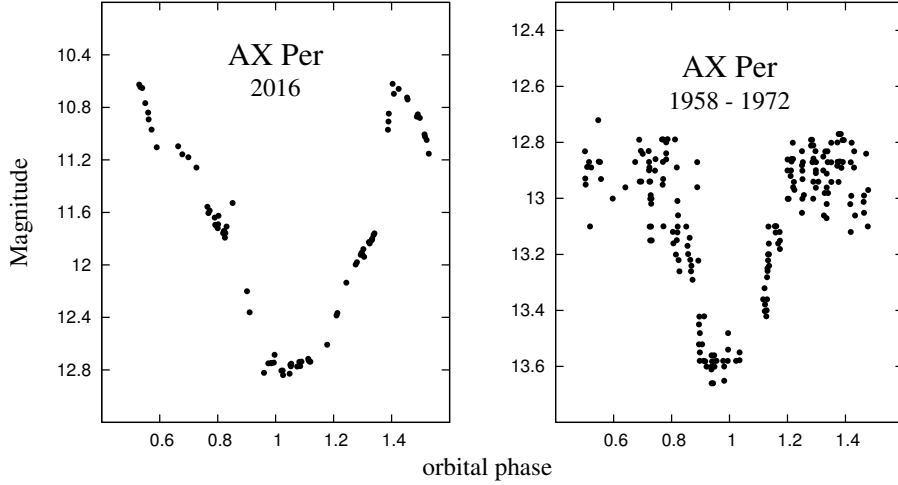


**Figure 31.** A comparison between the shape of the 2016 eclipse during the current active phase and eclipses during the 1958-1972 quiescent period (data are from Myalkovskij, 1977).

2018 ( $\varphi \sim 0.86$ ) showing a broad descending branch. Although our observations end before the predicted eclipse time, it seems that the light minimum precedes this position (Fig. 29). In general, the LC profile changes from cycle to cycle and is dependent on the colour. Such the behaviour reflects complex and variable sources of radiation around the WD as well as within the circumbinary environment.

### 3.15. FG Ser

Variability of the symbiotic star FG Ser was discovered by Hoffmeister (1968). The star underwent an outburst in 1988 when its brightness increased by  $\Delta B \sim 3.5$  mag and peaked at  $B \sim 10$  on July 4, 1988 (Munari & Iijima, 1988). The next monitoring of the star's brightness showed multiple maxima and minima - eclipses (see Munari et al., 1995, and Fig. 32 here). Using the timing of three eclipses observed during 1989 – 1993 the authors determined the eclipse ephemeris as  $JD_{\text{Ecl.}} = 2448492(\pm 4) + (658 \pm 4) \times E$ .

During the quiescent phase, prior to the 1988 outburst, Kurochkin (1993) determined the ephemeris for regular brightness variations ( $B = 13\text{--}14.5$ ) to  $JD_{\text{Min}} = 2446590.9 + 630 \times E$  using the photographic plates from the Stern-

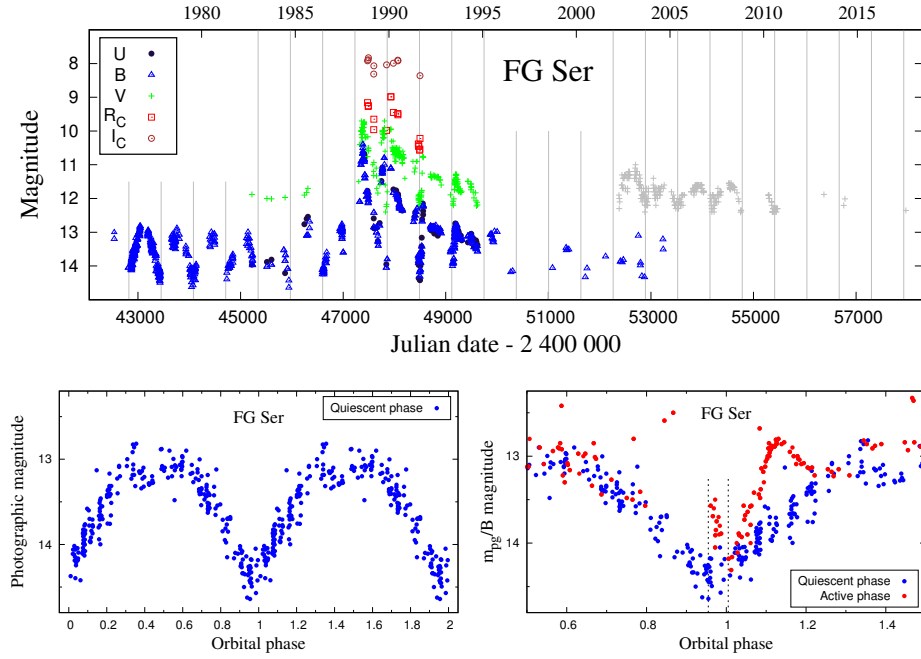


**Figure 32.** Top: As in Fig. 1, but for FG Ser. The vertical lines represent times of minima according to Eq. (3). The figure displays our photographic magnitudes from archives, data published by Kurochkin (1993) (shifted by -0.2 mag) and photographic and photoelectric data of Munari et al. (1992, 1995) (other colours). Compared are visual estimates from AAVSO (grey). Bottom: phase diagram of  $m_{pg}$  magnitudes during quiescent phase (left;  $JD < 2\,447\,000$ ) and its comparison with  $B$  measurements from the 1988-94 active phase (right).

berg Astronomical Institute archive (SAI; 1949-1987). He also determined the ephemeris of the secondary minimum, which is observed at the phase  $\varphi \sim 0.45$  with the depth of  $\sim 0.5$  mag. Using the same archive of photo-plates, but from 1901, the data of Munari et al. (1992, 1995) and new photometric observations, Shugarov et al. (2014) rectified the minima ephemeris to

$$JD_{\text{Min}} = 2\,443\,452(\pm 7) + (629.4 \pm 1.0) \times E \quad (3)$$

For the purpose of this paper, we remeasured magnitudes of FG Ser on photographic plates of the SAI archive (1955–1995; 256 plates). Our data are plotted together with those from literature in Fig. 32. During the quiescent phase ( $JD < 2\,447\,000$ ), their phase diagram with the ephemeris (3) shows typical wave-like orbitally-related variation with  $\Delta m_{pg} \sim 1.5$  mag, broad minimum around the inferior conjunction of the giant and a shallow  $\sim 0.3$  mag deep secondary minimum at  $\varphi \sim 0.4$ . During the active phase (1988-94), the minimum

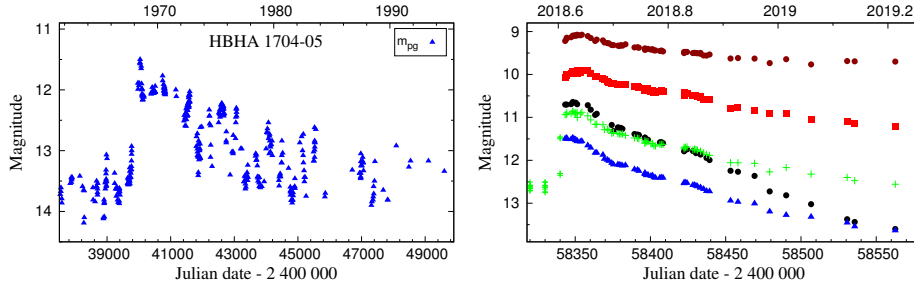


**Figure 33.** Left: Historical LC of HBHA 1704-05 obtained from the Moscow’s photographic plates archive. Right: Our  $UBVR_CI_C$  LCs measured from the maximum of the outburst, on August 12, 2018. Compared are the ASASSN  $V$  magnitudes prior to the outburst. Denotation of points as in Fig. 1.

(eclipse) became narrower and shifted its position after that from the quiescent phase by  $\sim 0.05 \times P_{\text{orb}}$  (bottom right panel of the figure), which prolongs the minima separation during the transition from quiescence to activity and during the decline from the outburst. This effect of apparent changes of orbital periods in symbiotic binaries was revealed by Skopal (1998). Here, we indicated this effect also for AE Ara (see Sect. 3.3).

### 3.16. HBHA 1704-05

The star HBHA 1704-05 was originally classified as an emission-line star (Kohoutek & Wehmeyer, 1999). On the basis of The All Sky Automated Survey for SuperNovae (ASAS-SN), the object was catalogued in the VSX as a semi-regular variable with a periodicity around 418 days. On August 11, 2018, Munari et al. (2018) reported that HBHA 1704-05 is coincident with the star TCP J19544251+1722281 (ASASSN-V J195442.95+172212.6), which brightened from  $V = 12.0$  on July 31.945, 2018 to  $V = 10.7$  on August 8.938, 2018, showing characteristics of a symbiotic star in outburst.<sup>9</sup> In the spectrum, they found features of an M-type giant, a strong nebular continuum with superposed emission lines of highly ionized elements (e.g., He II 4686 Å and [Ne V] 3426 Å), confirming the nature of HBHA 1704-05 as a symbiotic star in outburst. Photometric and spectroscopic monitoring of HBHA 1704-05 during the first month of its outburst was presented by Skopal et al. (2019).

We started to monitor HBHA 1704-05 on August 12, 2018, just after the discovery of its outburst. To obtain absolute values of its  $UBVR_CI_C$  magnitudes we used standard stars '120' and '123' as indicated on the AAVSO chart and the check star C = TYC 1620-2479 ( $\alpha_{2000} = 19^{\text{h}}54^{\text{m}}55^{\text{s}}$ ,  $\delta_{2000} = +17^{\circ}23'36''$ ). Using the standard stars  $\alpha$ , "b", "c" in the field of PU Vul and "a", "b", "c"

<sup>9</sup><http://www.cbat.eps.harvard.edu/unconf/followups/J19544251+1722281.html>

in the field of HM Sge (see charts of Henden & Munari, 2006), we determined the  $UBVR_CI_C$  magnitudes of the standard stars in the field of HBHA 1704-05. Resulting magnitudes represent mean values with *rms* errors obtained during 5 nights (see Table 1).

Our photometry of HBHA 1704-05 is depicted in Fig. 33. The right panel of the figure shows our multicolour CCD photometry during the current outburst. The LCs show a gradual decline, steepness of which depends on the colour. From the August's 2018 maximum to our last measurements during February 2019, the star's brightness decreased by  $\sim 2.6$ ,  $\sim 2.0$ ,  $\sim 1.5$ ,  $\sim 1.1$  and  $\sim 0.6$  mag in the  $U$ ,  $B$ ,  $V$ ,  $R_C$  and  $I_C$  filter, respectively. We also measured photographic magnitudes on the plates collected in the Moscow's photographic plates archive of the Sternberg Astronomical Institute of Moscow State University. These measurements revealed another 2-mag outburst lasting from 1968 to  $\sim 1975$  (left panel of the figure). A detailed analysis of LCs together with spectroscopic observations of HBHA 1704-05 is planned for another publication.

#### 4. Conclusions

In this paper, we present new multicolour long-term photometry of selected symbiotic stars. Main results of our monitoring program can be summarized as follows.

**EG And** persists in a quiescent phase. Our observations confirmed a double wave variation along the orbit in all  $UBVR_CI_C$  LCs. We also detected several light variations, with the most significant period around 28 days in the  $B$  LC.

**Z And** continues its active phase that started during September 2000. The amplitude of the brightness peaks, which appeared around  $\varphi = 0.5$  was gradually decreasing from  $U \sim 8.3$  in November 2011,  $\sim 9.1$  between February and May 2014 to  $\sim 9.6$  mag in June 2016. The recent outburst began in October 2017, peaking at  $U \sim 8.5$  mag in April 2018. We also indicated a periodic light variation with a  $\sim 58$ -day period, visible in our  $UBV$  data.

**AE Ara** came to quiescent phase from around 2016. During its recent active phase, from 2006 to 2016, we indicated a period of 850–860 days, which is distinctive larger than its orbital period of  $812 \pm 2$  days from light variations during preceding quiescence or  $803 \pm 9$  days from radial velocities. Such an apparent change in the orbital period is caused by the change of the ionization structure of the binary during quiescent and active phase (see Skopal, 1998).

**BF Cyg** remains at a high level of activity since its major outburst in 2006. The overall star's brightness was gradually declining until the eclipse position in 2014, when the trend turned into the opposite way, with the increasing delay of the minima position. During 2014, 2016 and 2018 the light minimum delayed by  $\sim 14$ ,  $\sim 17$  and  $\sim 20$  days after the inferior conjunction of the giant. The recent 2018-minimum ( $JD_{\text{Min}} \sim 2\,458\,230$ ) was followed by a  $\sim 0.3$  mag brightening peaked at  $U \sim 9.7$  mag on  $JD_{\text{Max}} \sim 2\,458\,360$ .

**CH Cyg** continues its active phase showing extremely complex photometric variability. Its brightness was gradually increasing to 2015 when reached a maximum of  $U \sim 7$  mag. During the following descending part of the  $UB(V)$  LCs CH Cyg underwent three bursts with a comparable amplitude of  $U \sim 1.7$  mag. During 2016, the light minima were shifted with increasing wavelength. Then CH Cyg reached its maximum at  $U \sim 6.4$  mag during the first half of 2018, being followed with a sharp minimum in May 2018 and continuing a  $\sim 2$  mag decrease in  $U$  by the end of 2018 (see Fig. 10).

**CI Cyg** experienced its last activity in the form of a double-peaked burst at the end of 2012. Then entered a quiescent phase showing pronounced orbitally-related light variation in the LCs. The recent broad minima in 2015 and 2017 differ in their position and profile for different colours. Secondary minima around  $\varphi \sim 0.6$  are present in  $BVR_CI_C$  LCs. A  $\sim 73$  days light variation can be recognized in the  $V$  LC (see Figs. 12 and 11).

**V1016 Cyg** continued a slow brightness decline in  $UBVR_C$  LCs by a few times 0.1 mag during our observing period (from March 2016), whereas the  $I_C$  LC reflects pulsations of the Mira-type giant with  $\Delta I_C \sim 0.7$  mag. A sudden drop in the  $U$  magnitude by  $\sim 0.17$  mag was measured around 2015.4 (see Fig. 15), confirming the previous finding by Arkhipova et al. (2016a,b). A decrease in the  $U - B$  and  $B - V$  colours (Fig. 16) can be in part caused by the overall star's brightness decline and a flux decrease of strong emission lines contributing to  $V$  and  $B$  passbands.

**V1329 Cyg** persists in quiescent phase showing well pronounced orbitally-related light variation with a decreasing amplitude at longer wavelengths. Their minima precede the inferior conjunction of the giant by  $\sim 0.1 \times P_{\text{orb}}$  (Fig. 17).

**AG Dra** continued its quasi-quiescent phase, during which the wave-like variability is occasionally interrupted by short-lasting ( $\lesssim 3$  months) bursts with  $\Delta U < 2$  mag. Bright bursts usually show a multi-peaked structure (see Figs. 18 and 19). We noticed a rather constant  $U - B$  colour during the last 2006-08 major outburst, while the  $B - V$  index does not show such feature. Similar plateau in the  $U - B$  LC was probably present also during the 1980-82 and 1994-95 major outbursts (see Fig. 20).

**RS Oph** persists at the stage between its recurrent outbursts. The  $BVR_CI_C$  LCs from the last 2006 eruption to the present suggest a smooth variation with the amplitude  $\Delta V \sim 0.3$  mag and a period of  $\sim 9.4$  years (Fig. 21). Rapid variability is detected in all filters. High-cadence measurements in  $B$  demonstrates a stochastic variability with  $\Delta B \sim 0.5$  mag on the time-scale of hours and  $\Delta B \sim 0.05 - 0.1$  mag on the time-scale of minutes (Fig. 22).

**AR Pav** reduced its out-of-eclipse activity from around 2004, showing only two  $\sim 0.5$  mag brightenings in 2013 and 2014 (Fig. 23). We determined positions of new minima from the epoch 71 to 78. All the available minima (1896.3 - 2018.8, Table 2) determine the linear ephemeris,  $JD_{\text{Min}} = 2411264.4(\pm 1.7) + (604.47 \pm 0.03) \times E$ . The corresponding  $O - C$  diagram indicates real systematic variation in the minima timing (Fig. 25).

**AG Peg** underwent its first Z And-type outburst in June 2015, after 165 years from its nova-like outburst in 1850 (Fig. 26). This change indicates the beginning of a new era in the AG Peg evolution. After about 1 year AG Peg came to a quiescent phase.

**AX Per** persists in a low-level active stage from about 2007. The LC profile varies from cycle to cycle and depends on the colour. For example, in 2016, the maximum in  $U$  preceded those in other filters by  $\sim 48$  days, while in 2017, maxima in  $U$  and  $B$  occurred at the same time, around  $\varphi = 0.4$ . The  $R_C$  LC shows secondary minima around  $\varphi = 0.45$ .

**FG Ser** was in quiescent phase from 1901 to 1987 as documented by re-measuring its archival photographic measurements. We determined a new ephemeris for its minima times,  $JD_{\text{Min}} = 2\,443\,452(\pm 7) + (629.4 \pm 1.0) \times E$ . During the active phase (1988-94), the minimum (eclipse) occurred by  $\sim 0.05 \times P_{\text{orb}}$  after the minima positions from quiescence.

**HBHA 1704-05** is the newly (August 9, 2018) discovered symbiotic star in outburst. Our  $UBVR_CI_C$  photometry shows that the current outburst is of Z And-type. By inspection of the Moscow's archive of photographic plates, we revealed another 2-mag-outburst of HBHA 1704-05 in 1968.

**Acknowledgements.** We thank the anonymous referee for constructive comments. Evgeni Kolotilov, Kirill Sokolovsky and Alexandra Zubareva are thanked for their assistance in acquisition of some data from the Moscow's photographic plates archive. Alisa Shchurova is thanked for her assistance in carrying out some CCD observations in the G2 pavilion within her PhD study. This work was supported by the Slovak Academy of Sciences grant VEGA No. 2/0008/17, by the Slovak Research and Development Agency under the contract No. APVV-15-0458 and by the Bulgarian Scientific Research Fund of the Ministry of Education and Science under the grants DN 08-1/2016 and DN 18-13/2017. Sergey Shugarov acknowledges the support from the Program of development of M.V. Lomonosov Moscow State University (Leading Scientific School 'Physics of stars, relativistic objects and galaxies'). We also acknowledge with thanks the variable star observations from the AAVSO International Database contributed by observers worldwide and used in this research.

## References

- Aaronson, M., Liebert, J., & Stocke, J., Discovery of carbon stars in the Draco dwarf spheroidal galaxy. 1982, *Astrophys. J.*, **254**, 507, DOI: 10.1086/159760
- Adamakis, S., Eyres, S. P. S., Sarkar, A., & Walsh, R. W., A pre-outburst signal in the long-term optical light curve of the recurrent nova RS Ophiuchi. 2011, *Mon. Not. R. Astron. Soc.*, **414**, 2195, DOI: 10.1111/j.1365-2966.2011.18536.x
- Allen, D. A. & Glass, I. S., Infrared photometry of southern emission-line stars. 1974, *Mon. Not. R. Astron. Soc.*, **167**, 337, DOI: 10.1093/mnras/167.2.337
- Andrews, P. J., Photometry of the eclipsing system AR Pavonis. 1974, *Mon. Not. R. Astron. Soc.*, **167**, 635, DOI: 10.1093/mnras/167.3.635

- Arhipova, V. P. & Mandel, O. E., On the Photometric History of V1329 Cygni = HBV 475. 1973, *Information Bulletin on Variable Stars*, **762**
- Arhipova, V. P., Esipov, V. F., Ikonnikova, N. P., & Komissarova, G. V., Photometric and spectroscopic evolution of the symbiotic nova V1016 Cygni after its outburst. 2008, *Astronomy Letters*, **34**, 474, DOI: 10.1134/S1063773708070062
- Arhipova, V. P., Taranova, O. G., Ikonnikova, N. P., et al., Symbiotic nova V1016 Cygni: Evolution of the dust envelope and the gaseous nebula. 2015, *Astronomy Letters*, **41**, 613, DOI: 10.1134/S1063773715110018
- Arhipova, V. P., Taranova, O. G., Ikonnikova, N. P., et al., Half a century after the outburst of the symbiotic nova V1016 Cyg. 2016a, *Baltic Astronomy*, **25**, 35
- Arhipova, V. P., Taranova, O. G., Ikonnikova, N. P., et al., VizieR Online Data Catalog: V1016 Cyg light curves and spectroscopy (Arhipova+, 2015). 2016b, *VizieR Online Data Catalog*, **904**
- Bacher, A., Kimeswenger, S., & Teutsch, P., Photometry from online Digitized Sky Survey plates. 2005, *Mon. Not. R. Astron. Soc.*, **362**, 542, DOI: 10.1111/j.1365-2966.2005.09329.x
- Belczyński, K., Mikołajewska, J., Munari, U., Ivison, R. J., & Friedjung, M., A catalogue of symbiotic stars. 2000, *Astron. Astrophys., Suppl.*, **146**, 407, DOI: 10.1051/aas:2000280
- Belyakina, T. S., The light variations of AG Peg from 1962 to 1967. 1970, *Astrofizika*, **6**, 49
- Belyakina, T. S., The symbiotic eclipsing variable CI cyg. Results of UBV and UB-VRI photometric observations in 1973-1988. 1991, *Bulletin Crimean Astrophysical Observatory*, **83**, 104
- Biller, B. A., Close, L. M., Li, A., et al., Resolving the Dusty Circumstellar Structure of the Enigmatic Symbiotic Star CH Cygni with the MMT Adaptive Optics System. 2006, *Astrophys. J.*, **647**, 464, DOI: 10.1086/505194
- Bogdanov, M. B. & Taranova, O. G., Variations of the parameters of the dust envelope of the symbiotic star CH Cygni. 2008, *Astronomy Reports*, **52**, 403, DOI: 10.1134/S1063772908050065
- Bondar', N. I. & Prokof'Eva, V. V., Nonradial pulsations of the hot component of the symbiotic star CH Cyg during its active phase. 2006, *Astronomy Reports*, **50**, 43, DOI: 10.1134/S1063772906010057
- Boyarchuk, A. A., The Nature of AG Pegasi. 1967, *Soviet Astronomy*, **11**, 8
- Boyarchuk, A. A., Esipov, V. F., & Moroz, V. I., The Continuous Spectrum of AG Pegasi. 1966, *Soviet Astronomy*, **10**, 331
- Brandi, E., Mikołajewska, J., Quiroga, C., et al., The spectroscopic orbits and other parameters of the symbiotic binary FN Sgr. 2005, *Astron. Astrophys.*, **440**, 239, DOI: 10.1051/0004-6361:20042552
- Brandi, E., Quiroga, C., Mikołajewska, J., Ferrer, O. E., & García, L. G., Spectroscopic orbits and variations of RS Ophiuchi. 2009, *Astron. Astrophys.*, **497**, 815, DOI: 10.1051/0004-6361/200811417

- Bruch, A., Optical observations of RS Ophiuchi in quiescence. 1986, *Astron. Astrophys.*, **167**, 91
- Bruch, A., Niehues, M., & Jones, A. F., The variable light curve of the eclipsing symbiotic star AR Pavonis. 1994, *Astron. Astrophys.*, **287**, 829
- Cariková, Z. & Skopal, A., Ionization structure of hot components in symbiotic binaries during active phases. 2012, *Astron. Astrophys.*, **548**, A21, DOI: 10.1051/0004-6361/201219221
- Corradi, R. L. M., Munari, U., Livio, M., et al., The Large-Scale Ionized Outflow of CH Cygni. 2001, *Astrophys. J.*, **560**, 912, DOI: 10.1086/323062
- Crowley, C. 2006, Red Giant Mass-Loss: Studying Evolved Stellar Winds with FUSE and HST/STIS, PhD thesis, School of Physics, Trinity College Dublin, Dublin 2, Ireland Ireland
- Esipov, V. F., Kolotilov, E. A., Mikolajewska, J., et al., Evolution of the Symbiotic Star AS338 after Its Strong Outburst in 1983. 2000, *Astronomy Letters*, **26**, 162, DOI: 10.1134/1.20379
- Fekel, F. C., Hinkle, K. H., Joyce, R. R., & Skrutskie, M. F., Infrared Spectroscopy of Symbiotic Stars. II. Orbits for Five S-Type Systems with Two-Year Periods. 2000a, *Astron. J.*, **120**, 3255, DOI: 10.1086/316872
- Fekel, F. C., Hinkle, K. H., Joyce, R. R., & Skrutskie, M. F., Infrared Spectroscopy of Symbiotic Stars. III. First Orbits for Three S-Type Systems. 2001, *Astron. J.*, **121**, 2219, DOI: 10.1086/319966
- Fekel, F. C., Hinkle, K. H., Joyce, R. R., & Wood, P. R., Infrared Spectroscopy of Symbiotic Stars. VIII. Orbits for Three S-Type Systems: AE Arae, Y Coronae Australis, and SS 73-147. 2010, *Astron. J.*, **139**, 1315, DOI: 10.1088/0004-6256/139/4/1315
- Fekel, F. C., Joyce, R. R., Hinkle, K. H., & Skrutskie, M. F., Infrared Spectroscopy of Symbiotic Stars. I. Orbits for Well-Known S-Type Systems. 2000b, *Astron. J.*, **119**, 1375, DOI: 10.1086/301260
- Fernandez-Castro, T., Gonzalez-Riestra, R., Cassatella, A., Taylor, A. R., & Seaquist, E. R., The active phase of the hot component of Z Andromedae. 1995, *Astrophys. J.*, **442**, 366, DOI: 10.1086/175446
- Formiggini, L. & Leibowitz, E. M., The historical light curve of the symbiotic star AG Draconis: intense, magnetically induced cyclic activity. 2012, *Mon. Not. R. Astron. Soc.*, **422**, 2648, DOI: 10.1111/j.1365-2966.2012.20829.x
- Gális, R., Hric, L., Friedjung, M., & Petrík, K., Resonances as the general cause of the outbursts in the symbiotic system AG Draconis. 1999, *Astron. Astrophys.*, **348**, 533
- González-Riestra, R., Selvelli, P., & Cassatella, A., XMM-Newton observations of RR Telescopii: evidence for wind signatures and shocked gas emission. 2013, *Astron. Astrophys.*, **556**, A85, DOI: 10.1051/0004-6361/201321358
- González-Riestra, R., Viotti, R., Iijima, T., & Greiner, J., IUE observations of the high-velocity symbiotic star AG Draconis. III. A compendium of 17 years of UV monitoring, and comparison with optical and X-ray observations. 1999, *Astron. Astrophys.*, **347**, 478

- Grygar, J., Hric, L., Chochol, D., & Mammano, A., The Symbiotic Variable V 1329 Cygni (= HBV 475)- a Decade After Its Discovery. 1979, *Bulletin of the Astronomical Institutes of Czechoslovakia*, **30**, 308
- Hachisu, I., Kato, M., Kiyota, S., et al., Optical Light Curves of RS Oph (2006) and Hydrogen Burning Turnoff. 2008, in *Astronomical Society of the Pacific Conference Series*, Vol. **401**, *RS Ophiuchi (2006) and the Recurrent Nova Phenomenon*, ed. A. Evans, M. F. Bode, T. J. O'Brien, & M. J. Darnley, 206
- Harvey, P. M., Infrared variability of V1016 Cygni. 1974, *Astrophys. J.*, **188**, 95, DOI: 10.1086/152689
- Henden, A. & Munari, U., UBVR(I)C photometric comparison sequences for symbiotic stars. 2000, *Astron. Astrophys., Suppl.*, **143**, 343, DOI: 10.1051/aas:2000183
- Henden, A. & Munari, U., UBVR(I)C photometric sequences for symbiotic stars. III. 2006, *Astron. Astrophys.*, **458**, 339, DOI: 10.1051/0004-6361:20065662
- Henden, A. & Munari, U., Multi-Epoch UBVRcIc Photometric Catalog of Symbiotic Stars. 2008, *Baltic Astronomy*, **17**, 293
- Hinkle, K. H., Fekel, F. C., & Joyce, R. R., Infrared Spectroscopy of Symbiotic Stars. VII. Binary Orbit and Long Secondary Period Variability of CH Cygni. 2009, *Astrophys. J.*, **692**, 1360, DOI: 10.1088/0004-637X/692/2/1360
- Hoffmeister, C., Mitteilungen über neuentdeckte Veränderliche Sterne (S 10153- S 10375). 1968, *Astronomische Nachrichten*, **290**, 277, DOI: 10.1002/asna.19672900512
- Hric, L., Gális, R., Leedjäv, L., Burmeister, M., & Kundra, E., Outburst activity of the symbiotic system AG Dra. 2014, *Mon. Not. R. Astron. Soc.*, **443**, 1103, DOI: 10.1093/mnras/stu1162
- Hric, L. & Skopal, A., Call for a Campaign of Long-Term Photometry of Symbiotic Stars. 1989, *Information Bulletin on Variable Stars*, **3364**
- Iijima, T., Eclipsing phenomena of the symbiotic star CH Cygni. 1998, *Mon. Not. R. Astron. Soc.*, **297**, 77, DOI: 10.1046/j.1365-8711.1998.01452.x
- Iijima, T., BF Cygni. 2006, *Central Bureau Electronic Telegrams*, **633**
- Iijima, T., A New Active Stage of the Symbiotic Star CH Cygni. 2017, *The Astronomer's Telegram*, **10142**
- Jacchia, L., Notes on Variable Stars. ;. 1941, *Harvard College Observatory Bulletin*, **915**, 17
- Jurdana-Šepić, R. & Munari, U., Symbiotic Stars on Asiago Archive Plates. 2010, *Publ. Astron. Soc. Pac.*, **122**, 35, DOI: 10.1086/650319
- Karovska, M., Gaetz, T. J., Carilli, C. L., et al., A Precessing Jet in the CH Cyg Symbiotic System. 2010, *Astrophys. J., Lett.*, **710**, L132, DOI: 10.1088/2041-8205/710/2/L132
- Kenyon, S. J. 1986, *The symbiotic stars* (Cambridge: Cambridge University Press)
- Kenyon, S. J. & Fernandez-Castro, T., The cool components of symbiotic stars. I - Optical spectral types. 1987, *Astron. J.*, **93**, 938, DOI: 10.1086/114379

- Kenyon, S. J. & Garcia, M. R., EG Andromedae: A New Orbit and Additional Evidence for a Photoionized Wind. 2016, *Astron. J.*, **152**, 1, DOI: 10.3847/0004-6256/152/1/1
- Kenyon, S. J., Mikolajewska, J., Mikolajewski, M., Polidan, R. S., & Slovak, M. H., Evolution of the symbiotic binary system AG Pegasi - The slowest classical nova eruption ever recorded. 1993, *Astron. J.*, **106**, 1573, DOI: 10.1086/116749
- Kenyon, S. J., Proga, D., & Keyes, C. D., The Continuing Slow Decline of AG Pegasi. 2001, *Astron. J.*, **122**, 349, DOI: 10.1086/321107
- Kenyon, S. J. & Webbink, R. F., The nature of symbiotic stars. 1984, *Astrophys. J.*, **279**, 252, DOI: 10.1086/161888
- Kinemuchi, K., Harris, H. C., Smith, H. A., et al., The Variable Stars of the Draco Dwarf Spheroidal Galaxy: Revisited. 2008, *Astron. J.*, **136**, 1921, DOI: 10.1088/0004-6256/136/5/1921
- Kohoutek, L., HBV475: a New Peculiar Emission Object in Cygnus. 1969, *Information Bulletin on Variable Stars*, **384**
- Kohoutek, L. & Wehmeyer, R., Catalogue of H-alpha emission stars in the Northern Milky Way. 1999, *Astron. Astrophys., Suppl.*, **134**, 255, DOI: 10.1051/aas:1999101
- Kondratyeva, L. N., Rspaev, F. K., Krugov, M. A., & Serebryanskiy, A. V., Active Stage of the Object CH Cyg B in 2014-2015. 2017, *Astrophysics*, **60**, 153, DOI: 10.1007/s10511-017-9471-z
- Kurochkin, N. E., A new type of cataclysmic variability: FG serpentis and QW sagittae. 1993, *Astronomical and Astrophysical Transactions*, **3**, 295, DOI: 10.1080/10556799308230567
- Leedjäv, L., Gális, R., Hric, L., Merc, J., & Burmeister, M., Spectroscopic view on the outburst activity of the symbiotic binary AG Draconis. 2016, *Mon. Not. R. Astron. Soc.*, **456**, 2558, DOI: 10.1093/mnras/stv2807
- Leibowitz, E. M. & Formigini, L., Multiperiodic variations in the last 104-yr light curve of the symbiotic star BF Cyg. 2006, *Mon. Not. R. Astron. Soc.*, **366**, 675, DOI: 10.1111/j.1365-2966.2005.09895.x
- Leibowitz, E. M. & Formigini, L., Activity cycle of the giant star of Z Andromedae and its spin period. 2008, *Mon. Not. R. Astron. Soc.*, **385**, 445, DOI: 10.1111/j.1365-2966.2008.12847.x
- Lundmark, K., Ein neuer Veränderlicher vom P Cygni-Typus. 1921, *Astronomische Nachrichten*, **213**, 93, DOI: 10.1002/asna.19212130604
- Matthews, L. D. & Karovska, M., First Resolved Images of the Mira AB Symbiotic Binary at Centimeter Wavelengths. 2006, *Astrophys. J., Lett.*, **637**, L49, DOI: 10.1086/500303
- Mayall, M. W. & Shapley, H., A new eclipsing star of unusual character. 1937, *Annals of Harvard College Observatory*, **105**, 491
- McCuskey, S., Activity in H $\alpha$  emission object. 1965, *IAU Circ.*, **1916**

- McKeever, J., Lutz, J., Wallerstein, G., Munari, U., & Siviero, A., High-Dispersion Spectroscopy of BF Cygni at the Beginning of the 2006 Outburst. 2011, *Publ. Astron. Soc. Pac.*, **123**, 1062, DOI: 10.1086/662076
- Meinunger, L., Discovery of a Period in the Symbiotic Star AG Draconis. 1979, *Information Bulletin on Variable Stars*, **1611**
- Mikayilov, K. M., Rustamov, B. N., Alakbarov, I. A., & Rustamova, A. B., Rapid Spectral Variability of the Symbiotic Star CH Cyg During One Night. 2017, in Astronomical Society of the Pacific Conference Series, Vol. **510**, *Stars: From Collapse to Collapse*, ed. Y. Y. Balega, D. O. Kudryavtsev, I. I. Romanyuk, & I. A. Yakunin, 170
- Mikolajewska, J. & Kenyon, S. J., On the nature of the symbiotic binary AX Persei. 1992, *Astron. J.*, **103**, 579, DOI: 10.1086/116085
- Mikolajewska, J., Quiroga, C., Brandi, E., et al., The Spectroscopic Orbit and Other Parameters of AE Arae. 2003, in Astronomical Society of the Pacific Conference Series, Vol. **303**, *Symbiotic Stars Probing Stellar Evolution*, ed. R. L. M. Corradi, J. Mikolajewska, & T. J. Mahoney, 147
- Mikolajewska, J., Selvelli, P. L., & Hack, M., IUE low resolution observations of the symbiotic star CH Cygni in 1979-1986. 1988, *Astron. Astrophys.*, **198**, 150
- Motta, M. E. & Motta, A., Ultra-Short Variability in CH Cygni. 2000, *Journal of the American Association of Variable Star Observers (JAAVSO)*, **28**, 106
- Muerset, U., Nussbaumer, H., Schmid, H. M., & Vogel, M., Temperature and luminosity of hot components in symbiotic stars. 1991, *Astron. Astrophys.*, **248**, 458
- Mukai, K., Kennea, J. A., Luna, G. J. M., & Sokoloski, J. L., Increased X-ray Activities of the Symbiotic Star, CH Cygni. 2009, *The Astronomer's Telegram*, **2245**
- Munari, U., BVI Photometry of the Symbiotic Star C-1 in the Draco Dwarf Galaxy. 1991, *Information Bulletin on Variable Stars*, **3605**
- Munari, U., Dallaporta, S., Valisa, P., et al., HBHa 1704-05: a bright and newly discovered symbiotic star, currently undergoing an "hot-type" outburst. 2018, *The Astronomer's Telegram*, **11937**
- Munari, U. & Iijima, T., AS 296. 1988, *IAU Circ.*, **4622**
- Munari, U., Maitan, A., Moretti, S., & Tomaselli, S., 500 days of Stromgren b, y and narrow-band [OIII], H  $\alpha$  photometric evolution of gamma-ray Nova Del 2013 (=V339 Del). 2015, *New Astron.*, **40**, 28, DOI: 10.1016/j.newast.2015.03.008
- Munari, U., Siviero, A., Corradi, R. L. M., et al., AX Persei. 2010, *Central Bureau Electronic Telegrams*, **2555**
- Munari, U., Siviero, A., Dallaporta, S., et al., AX Persei. 2009a, *Central Bureau Electronic Telegrams*, **1757**
- Munari, U., Siviero, A., Moretti, S., et al., BF Cygni. 2006, *Central Bureau Electronic Telegrams*, **596**
- Munari, U., Siviero, A., Ochner, P., et al., Long term BVRIC photometry of carbon and symbiotic stars in the Draco dwarf galaxy. 2008, *Information Bulletin on Variable Stars*, **5855**

- Munari, U., Siviero, A., Ochner, P., et al., The 2006-2008 Outburst of AG Draconis. 2009b, *Publ. Astron. Soc. Pac.*, **121**, 1070, DOI: 10.1086/606169
- Munari, U., Whitelock, P. A., Gilmore, A. C., et al., The ongoing outburst of the eclipsing symbiotic nova AS 296 - The first 1200 days. 1992, *Astron. J.*, **104**, 262, DOI: 10.1086/116238
- Munari, U., Yudin, B. F., Kolotilov, E. A., & Gilmore, A. C., The ongoing outburst of the eclipsing symbiotic nova AS 296 = FG SER. 2: UBV-JHKL photometry over days 1200-2300. 1995, *Astron. J.*, **109**, 1740, DOI: 10.1086/117403
- Mürset, U. & Schmid, H. M., Spectral classification of the cool giants in symbiotic systems. 1999, *Astron. Astrophys., Suppl.*, **137**, 473, DOI: 10.1051/aas:1999105
- Myalkovskij, M. I., Observations of three symbiotic stars: Z Andromedae, AX Persei, and CI Cygni. 1977, *Peremennye Zvezdy Prilozhenie*, **3**, 71
- Nussbaumer, H. & Vogel, M., A new approach to symbiotic stars. 1987, *Astron. Astrophys.*, **182**, 51
- Nussbaumer, H. & Vogel, M., Z Andromedae and the symbiotic phenomenon. 1989, *Astron. Astrophys.*, **213**, 137
- Oliveresen, N. A., Anderson, C. M., Stencel, R. E., & Slovak, M. H., Observational studies of the symbiotic stars. III High-dispersion IUE and H-alpha observations of EG Andromedae. 1985, *Astrophys. J.*, **295**, 620, DOI: 10.1086/163404
- Oppenheimer, B. & Mattei, J. A., An Analysis of Longterm AAVSO Observations of the Recurrent Nova RS Ophiuchi. 1993, in Bulletin of the American Astronomical Society, Vol. **25**, *American Astronomical Society Meeting Abstracts*, 1378
- Parimucha, S., Arkhipova, V. P., Chochol, D., et al., Long-term photometry of the symbiotic nova V1016 Cyg. 2000, *Contributions of the Astronomical Observatory Skalnaté Pleso*, **30**, 99
- Parimucha, Š., Chochol, D., Pribulla, T., Buson, L. M., & Vittone, A. A., Multiwavelength evidence for a 15-year periodic activity in the symbiotic nova V1016 Cygni. 2002, *Astron. Astrophys.*, **391**, 999, DOI: 10.1051/0004-6361:20020847
- Pedretti, E., Monnier, J. D., Lacour, S., et al., Detection of non-radial pulsation and faint companion in the symbiotic star CH Cyg. 2009, *Mon. Not. R. Astron. Soc.*, **397**, 325, DOI: 10.1111/j.1365-2966.2009.14906.x
- Percy, J. R., Wilson, J. B., & Henry, G. W., Long-Term VRI Photometry of Small-Amplitude Red Variables. I. Light Curves and Periods. 2001, *Publ. Astron. Soc. Pac.*, **113**, 983, DOI: 10.1086/322153
- Pojmanski, G., The All Sky Automated Survey. Catalog of Variable Stars. I. 0 h - 6 hQuarter of the Southern Hemisphere. 2002, *Acta Astronomica*, **52**, 397
- Pucinskas, A., On some periodicity phenomena in symbiotic stars. 1970, *Vilnius Astronomijos Observatorijos Biuletėnis*, **27**, 24
- Ramsay, G., Sokoloski, J. L., Luna, G. J. M., & Nuñez, N. E., Swift observations of the 2015 outburst of AG Peg - from slow nova to classical symbiotic outburst. 2016, *Mon. Not. R. Astron. Soc.*, **461**, 3599, DOI: 10.1093/mnras/stw1546
- Schaefer, B. E., RS Ophiuchi. 2004, *IAU Circ.*, **8396**

- Schild, H., Boyle, S. J., & Schmid, H. M., Infrared spectroscopy of symbiotic stars - Carbon abundances and C-12/C-13 isotopic ratios. 1992, *Mon. Not. R. Astron. Soc.*, **258**, 95, DOI: 10.1093/mnras/258.1.95
- Schild, H., Dumm, T., Mürset, U., et al., High resolution spectroscopy of symbiotic stars. VI. Orbital and stellar parameters for AR Pavonis. 2001, *Astron. Astrophys.*, **366**, 972, DOI: 10.1051/0004-6361:20000338
- Schild, H. & Schmid, H. M., Spectropolarimetry and nebular geometry of the symbiotic star HBV 475. 1997, *Astron. Astrophys.*, **324**, 606
- Schmid, H. M. & Schild, H., Spectropolarimetry of symbiotic stars: AG Draconis. 1997, *Astron. Astrophys.*, **321**, 791
- Seaquist, E. R., Taylor, A. R., & Button, S., A radio survey of symbiotic stars. 1984, *Astrophys. J.*, **284**, 202, DOI: 10.1086/162399
- Shugarov, S., Kolotilov, E., Komissarova, G., Skopal, A., & Zemko, P., Photometric Activity of the Symbiotic Star CH Cyg during 2008–2011. 2012, *Baltic Astronomy*, **21**, 184, DOI: 10.1515/astro-2017-0375
- Shugarov, S., Kolotilov, E., & Sokolovsky, K., Improvement of the orbital period of the symbiotic binary FG Ser by using archival photographic and new photoelectric observations. 2014, in *Astroplate 2014*, 115–118
- Shugarov, S., Skopal, A., Sekeráš, M., Komissarova, G., & Wolf, M., Rapid Photometric Variability Of The Symbiotic System CH Cyg During 2008-15. 2015, in *EAS Publications Series*, Vol. **71**, *EAS Publications Series*, 107–108
- Siviero, A., Munari, U., Dallaporta, S., et al., The ongoing 2008-09 outburst of CI Cyg. 2009, *Mon. Not. R. Astron. Soc.*, **399**, 2139, DOI: 10.1111/j.1365-2966.2009.15414.x
- Skopal, A., New Ephemeris of the Eclipsing Symbiotic Star AX Per. 1991, *Information Bulletin on Variable Stars*, **3603**
- Skopal, A., Is the symbiotic binary EG And an eclipsing system? 1997, *Astron. Astrophys.*, **318**, 53
- Skopal, A., On the nature of apparent changes of the orbital period in symbiotic binaries. 1998, *Astron. Astrophys.*, **338**, 599
- Skopal, A., What mimics the reflection effect in symbiotic binaries? 2001, *Astron. Astrophys.*, **366**, 157, DOI: 10.1051/0004-6361:20000217
- Skopal, A., Disentangling the composite continuum of symbiotic binaries. I. S-type systems. 2005, *Astron. Astrophys.*, **440**, 995, DOI: 10.1051/0004-6361:20034262
- Skopal, A., Broad H $\alpha$  wings from the optically thin stellar wind of the hot components in symbiotic binaries. 2006, *Astron. Astrophys.*, **457**, 1003, DOI: 10.1051/0004-6361:20064935
- Skopal, A., How to Understand the Light Curves of Symbiotic Stars. 2008, *Journal of the American Association of Variable Star Observers (JAAVSO)*, **36**, 9
- Skopal, A., Bode, M. F., Crocker, M. M., et al., The symbiotic star CH Cygni - IV. Basic kinematics of the circumstellar matter during active phases. 2002, *Mon. Not. R. Astron. Soc.*, **335**, 1109, DOI: 10.1046/j.1365-8711.2002.05715.x

- Skopal, A., Bode, M. F., Lloyd, H. M., & Tamura, S., Eclipses in the symbiotic system CH CYG. 1996, *Astron. Astrophys.*, **308**, L9
- Skopal, A., Chochol, D., Pribulla, T., & Vanko, M., UBV Photometry of the Symbiotic Star Z And During its 2000 Outburst. 2000a, *Information Bulletin on Variable Stars*, **5005**
- Skopal, A., Djurašević, G., Jones, A., et al., A photometric study of the eclipsing symbiotic binary ARPavonis. 2000b, *Mon. Not. R. Astron. Soc.*, **311**, 225, DOI: 10.1046/j.1365-8711.2000.03040.x
- Skopal, A., Kohoutek, L., Jones, A., & Drechsel, H., The historical, 1889-2002, light curve of the eclipsing symbiotic binary AR Pav. 2001a, *Information Bulletin on Variable Stars*, **5195**
- Skopal, A. & Pribulla, T., The first detection of the bipolar jets from the symbiotic prototype Z And. 2006, *The Astronomer's Telegram*, **882**
- Skopal, A., Pribulla, T., Vaňko, M., et al., Photometry of symbiotic stars. XI. EG And, Z And, BF Cyg, CH Cyg, CI Cyg, V1329 Cyg, TX CVn, AG Dra, RW Hya, AR Pav, AG Peg, AX Per, QW Sge, IV Vir and the LMXB V934 Her. 2004, *Contributions of the Astronomical Observatory Skalnaté Pleso*, **34**, 45
- Skopal, A., Sekeráš, M., Shugarov, S., & Shagatova, N., New burst of the active symbiotic star BF Cyg at the beginning of 2017. 2017a, *The Astronomer's Telegram*, **10086**
- Skopal, A., Sekeráš, M., González-Riestra, R., & Viotti, R. F., The origin of the supersoft X-ray-optical/UV flux anticorrelation in the symbiotic binary AG Draconis. 2009, *Astron. Astrophys.*, **507**, 1531, DOI: 10.1051/0004-6361/200811418
- Skopal, A., Sekeráš, M., Kundra, E., et al., First glance to the recently discovered symbiotic star HBHA 1704-05 during its current outburst. 2019, *Contrib. Astron. Obs. Skalnaté Pleso*, **49**, 1
- Skopal, A., Shugarov, S., & Chochol, D., Recent optical burst of the symbiotic star CH Cygni. 2010, *The Astronomer's Telegram*, **2394**
- Skopal, A., Shugarov, S., Vaňko, M., et al., Recent photometry of symbiotic stars. 2012, *Astronomische Nachrichten*, **333**, 242, DOI: 10.1002/asna.201111655
- Skopal, A., Shugarov, S. Y., Sekeráš, M., et al., New outburst of the symbiotic nova AG Pegasi after 165 yr. 2017b, *Astron. Astrophys.*, **604**, A48, DOI: 10.1051/0004-6361/201629593
- Skopal, A., Tarasova, T. N., Cariková, Z., et al., Formation of a disk structure in the symbiotic binary AX Persei during its 2007-10 precursor-type activity. 2011, *Astron. Astrophys.*, **536**, A27, DOI: 10.1051/0004-6361/201116969
- Skopal, A., Tarasova, T. N., Wolf, M., Dubovský, P. A., & Kudzej, I., Repeated Transient Jets from a Warped Disk in the Symbiotic Prototype Z And: A Link to the Long-lasting Active Phase. 2018, *Astrophys. J.*, **858**, 120, DOI: 10.3847/1538-4357/aabc11

- Skopal, A., Teodorani, M., Errico, L., et al., A photometric and spectroscopic study of the eclipsing symbiotic binary AX Persei. 2001b, *Astron. Astrophys.*, **367**, 199, DOI: 10.1051/0004-6361:20000413
- Skopal, A., Vaňko, M., Pribulla, T., et al., Recent photometry of symbiotic stars. 2007, *Astronomische Nachrichten*, **328**, 909, DOI: 10.1002/asna.200710822
- Skopal, A., Vittone, A., Errico, L., et al., A photometric and spectroscopic study of the symbiotic binary BF CYG. 1997, *Mon. Not. R. Astron. Soc.*, **292**, 703, DOI: 10.1093/mnras/292.3.703
- Sokoloski, J. L. & Kenyon, S. J., CH Cygni. I. Observational Evidence for a Disk-Jet Connection. 2003, *Astrophys. J.*, **584**, 1021, DOI: 10.1086/345901
- Sokoloski, J. L., Zamanov, R., Stoyanov, K., Bryson, S., & Still, M., Cessation of optical flickering from the symbiotic star CH Cygni. 2010, *The Astronomer's Telegram*, **2707**
- Sokolovsky, K. V., Kolesnikova, D. M., Zubareva, A. M., Samus, N. N., & Antipin, S. V., Variable stars identification in digitized photographic data. 2016, *arXiv e-prints* [[arXiv]1605.03571]
- Stienon, F. M., Chartrand, III, M. R., & Shao, C. Y., The emission-line variable HBV 475. 1974, *Astron. J.*, **79**, 47, DOI: 10.1086/111529
- Stoyanov, K., Zamanov, R., & Sokoloski, J. L., Optical flickering from the symbiotic star CH Cygni is still missing. 2012, *The Astronomer's Telegram*, **4316**
- Stoyanov, K. A., Martí, J., Zamanov, R., et al., Optical flickering of the symbiotic star CH Cyg. 2018, *Bulgarian Astronomical Journal*, **28**, 42
- Taranova, O. G. & Shenavrin, V. I., Unusual infrared fading of CH Cygni in 2006. 2007, *Astronomy Letters*, **33**, 531, DOI: 10.1134/S106377370708004X
- Tomov, T. V., Stoyanov, K. A., & Zamanov, R. K., AG Pegasi - now a classical symbiotic star in outburst? 2016, *Mon. Not. R. Astron. Soc.*, **462**, 4435, DOI: 10.1093/mnras/stw2012
- Vaňko, M., Kollár, V., Komžík, R., Koza, J., & Pribulla, T., Photoelectric photometry era at the Astronomical Institute of the Slovak Academy of Sciences III. Fast photometry. 2015, *Contributions of the Astronomical Observatory Skalnaté Pleso*, **45**, 99
- Vaňko, M., Komžík, R., Kollár, V., & Sekeráš, M., Photoelectric photometry era at the Astronomical Institute of the Slovak Academy of Sciences I. Instrumentation, colour system and extinction. 2014a, *Contributions of the Astronomical Observatory Skalnaté Pleso*, **44**, 77
- Vaňko, M., Komžík, R., Kollár, V., & Sekeráš, M., Photoelectric photometry era at the Astronomical Institute of the Slovak Academy of Sciences II. Software and reduction techniques. 2014b, *Contributions of the Astronomical Observatory Skalnaté Pleso*, **44**, 91
- Waagen, E. O., Very rare outburst of the symbiotic variable AG Peg. 2015, *AAVSO Alert Notice*, **521**

- Wallerstein, G., Munari, U., Siviero, A., Dallaporta, S., & Dalmeri, I., The Spectrum and Light Curve of CH Cygni during its Recent Broad Minimum. 2010, *Publ. Astron. Soc. Pac.*, **122**, 12, DOI: 10.1086/648563
- Webster, B. L. & Allen, D. A., Symbiotic stars and dust. 1975, *Mon. Not. R. Astron. Soc.*, **171**, 171, DOI: 10.1093/mnras/171.1.171
- Wilson, R. E. & Vaccaro, T. R., Ellipsoidal variation in EG Andromedae. 1997, *Mon. Not. R. Astron. Soc.*, **291**, 54, DOI: 10.1093/mnras/291.1.54
- Worters, H. L., Eyres, S. P. S., Bromage, G. E., & Osborne, J. P., Resumption of mass accretion in RS Oph. 2007, *Mon. Not. R. Astron. Soc.*, **379**, 1557, DOI: 10.1111/j.1365-2966.2007.12066.x
- Yudin, B. F., Kolotilov, E. A., Shenavrin, V. I., Tatarnikova, A. A., & Tatarnikov, A. M., UBV photometry of the classical symbiotic star BF Cygni. 2005, *Astronomical and Astrophysical Transactions*, **24**, 447, DOI: 10.1080/10556790500524155
- Zamanov, R., Latev, G., Boeva, S., et al., Optical flickering of the recurrent nova RS Ophiuchi: amplitude-flux relation. 2015, *Mon. Not. R. Astron. Soc.*, **450**, 3958, DOI: 10.1093/mnras/stv873



PRÁCE ASTRONOMICKÉHO OBSERVATÓRIA  
NA SKALNATOM PLESE  
XLIX, číslo 1

Zostavovateľ:	RNDr. Richard Komžík, CSc.
Vedecký redaktor:	RNDr. Augustín Skopal, DrSc.
Vydal:	Astronomický ústav SAV, Tatranská Lomnica
IČO vydavateľa:	00 166 529
Periodicita:	2-krát ročne
ISSN (on-line verzia):	1336-0337
CODEN:	CAOPF8
Rok vydania:	2019
Počet strán:	68

Contributions of the Astronomical Observatory Skalnaté Pleso are processed using  
 $\LaTeX$  2 $\epsilon$  CAOSP DocumentClass file 3.06 ver. 2017.